PSI Ber. 98-06

PAUL SCHERRER INSTITUT

PSI Bericht Nr. 98-06
August 1998
ISSN 1019-0643

Solid State Research at Large Facilities

Physics and Technology of Spallation Neutron Sources

G. S. Bauer

Paul Scherrer Institut
CH - 5232 Villigen PSI
Telefon 056 310 21 11
Telefax 056 310 21 99

PSI-Bericht Nr. 98-06

Physics and Technology of Spallation Neutron Sources

G.S. Bauer
Spallation Neutron Source Division
Paul Scherrer Institut
CH-5232 Villigen PSI, Switzerland
Guenter.Bauer@psi.ch

Lecture notes of a course given at the

1998 Frédéric Joliot Summer School
in Cadarache, France, August 16 - 27, 1998
intended for publication, in revised form, in a Special Issue of
Nuclear Instruments and Methods A.

Paul Scherrer Institut
Solid State Research at Large Facilities
August 1998

Physics and Technology of Spallation Neutron Sources[1]

G.S. Bauer
Spallation Neutron Source Division
Paul Scherrer Institut
CH-5232 Villigen PSI, Switzerland
Guenter.Bauer@psi.ch

Abstract

Next to fission and fusion, spallation is an efficient process for releasing neutrons from nuclei. Unlike the other two reactions, it is an endothermal process and can, therefore, not be used per se in energy generation. In order to sustain a spallation reaction, an energetic beam of particles, most commonly protons, must be supplied onto a heavy target. Spallation can, however, play an important role as a source of neutrons whose flux can be easily controlled via the driving beam. Up to a few GeV of energy, the neutron production is roughly proportional to the beam power. Although sophisticated Monte Carlo codes exist to compute all aspects of a spallation facility, many features can be understood on the basis of simple physics arguments. Technically a spallation facility is very demanding, not only because a reliable and economic accelerator of high power is needed to drive the reaction, but also, and in particular, because high levels of radiation and heat are generated in the target which are difficult to cope with. Radiation effects in a spallation environment are different from those commonly encountered in a reactor and are probably even more temperature dependent than the latter because of the high gas production rate. A commonly favored solution is the use of molten heavy metal targets. While radiation damage is not a problem in this case, except for the container, a number of other issues are discussed.

1. Introduction

Using medium energy particle bombardment of heavy metals to release neutrons is not a new idea. In fact, before large deposits of Uranium are were discovered in the US, a project called MTA was well advanced, which was designed to provide enough neutrons to convert ^{238}U into Plutonium for the nuclear weapons program. The project was given up when breeding in fission reactors became a more economic alternative. The recent revival of interest in spallation-based neutron sources has essentially two reasons:

- fission reactor technology is essentially neutron-poor, i.e. only few excess neutrons can be made available either for fertile-fissile conversion or for nuclear transmutation towards waste management. Furthermore, fast reactors, i.e. those with a hard neutron spectrum, or desired for many advanced technologies are difficult, because only metallic coolants can be used. Spallation, on the other hand, can generate high neutron densities and hard spectra, but has its own technological issues. In this context the experience that can be gained from research spallation sources may become very valuable.

- in the field of research neutron sources reactors have more or less reached their limits of thermal flux that can be generated with existing fuel technology due to power density problems in the core. A perspective for progress is seen in the spallation reaction for two reasons:

  - the lower heat release per neutron and the increased flexibility in materials choices, which might help to push time average fluxes to higher values than in fission reactors

  - the possibility of imposing a time structure on the neutron flux, which can lead to several orders of magnitude higher flux in the pulse than in the time average. Methods are being developed

[1] Lecture notes of a course given at the 1998 Frédéric Jolliot Summer School in Cadarache, France; intended for publication, in revised form, in a Special Issue of Nuclear Instruments and Methods A.

in the utilization of pulsed sources which essentially make use of the peak flux during most of the period between pulses by exploiting the energy-dependent flight time of neutrons from the moderator to detectors located several tens of meters away.

The principal design of a research spallation neutron source for neutron scattering is shown in Fig. 1-1. A medium energy proton beam is injected into a target in which fast neutron are generated. In order to provide neutrons useful for scattering experiments, they must be slowed down to the meV range by moderators placed near the target. Good neutronic coupling between these moderators and the target is, of course, an important design goal. In order to increase this coupling, the moderators are surrounded by a reflector, whose task is to scatter as many of the neutrons that would otherwise escape the moderators back into them. Neutrons to be used in the scattering experiments are transported outwards through the shielding by beam tubes viewing the moderators in a way that minimizes high energy and fast neutron as well as gamma ray contamination in the beam. Depending on the type of neutron source, the moderators will be laid out differently in order to achieve the kind of optimization desired by the users: For maximum time average flux the life time of the neutrons must be long, meaning that neutron absorption in the moderators and the reflector (and in the target as well) should be minimized. For this reason heavy water is commonly used as moderator and reflector alike. For very short pulses the moderators will be surrounded by absorbing material to avoid slow neutron return from the reflector, and, for the intermediate case of intense pulses with moderately good time structure, one will try to minimize moderation in the reflector material but not kill neutrons by placing absorbers around the moderator. So, spallation neutron sources offer a wide variety of choices and, of course, requite different technical solutions for different optimization criteria. A very important parameter in this context is the moderator temperature, which affects the spectral distribution as well as the pulse shape over a large energy range.

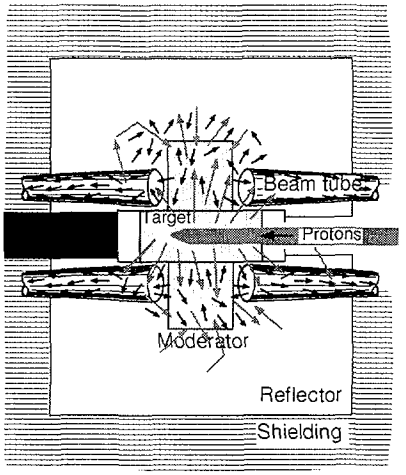

Figure 1-1: *Principal arrangement of target moderators and reflector in a spallation neutron source for neutron scattering*

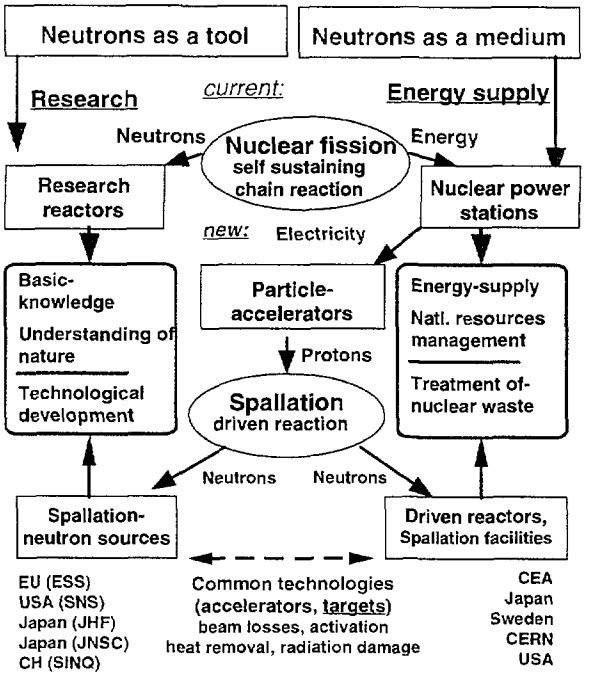

Figure 1-2: *Neutrons in science and economy*

As it was true in the development of reactors, where research facilities provided most of the information needed to develop reliable nuclear power stations, a similar symbiosis might also be in the interest of research spallation sources and new accelerator driven devices. This is shown schematically in Fig. 1.2. This present paper will first review some of the physics issues of neutron generations and moderation in order to provide a basic understanding of the design

decisions involved and, after giving an example each for a modern continuous and a pulsed research neutron source, discuss some technical issues related to the further development of spallation neutron sources. Most of these issues are relevant also in accelerator driven devices for nuclear power applications.

2. Neutrons from fission and spallation

The physics of spallation is being treated in detail in different lectures of this school. Here we give only a phenomenological description useful to visualize the underlying phenomena and to develop a feeling for the influence of the various parameters that govern the process.

2.1 The fission process

Since fission is an extremely well studied process, it may be worthwhile to point out some of the similarities and dissimilarities between fission and spallation:

The most common fission reactions are the ones resulting from the capture of a thermal or fast neutron in a so called "fissionable" nucleus. A compound nucleus forms, which is unstable against deformation. According to the "droplet" model, it breaks apart when the Coulomb repulsion between the two halves of the deformed nucleus equals the restoring force of the nuclear surface tension. Neutrons are occasionally freed during the scission process, but mainly result from evaporation from the fission fragments which are on the neutron-rich side of the nuclear stability curve and hence have an excess of internal energy.

The spectrum of neutrons obtained from nuclear fission is fairly well described by a Maxwellian distribution function:

$$n(E) = \frac{2 \cdot E^{1/2}}{\pi^{1/2} E_T^{3/2}} \exp\left(-\frac{E}{E_T}\right) \qquad (2.1)$$

Here, E_T has the meaning of the kinetic energy kT corresponding to a certain "temperature" of the nucleons in the nucleus. Values for E_T are 1.29 MeV for ^{235}U-fission and 1.33 MeV for ^{239}Pu fission representing temperatures of $1.14 \cdot 10^8$ K and $1.18 \cdot 10^8$ K, respectively. The mean energy of the neutron in the distribution (2.1) is

$$\overline{E} = 3/2\, E_T \qquad (2.2)$$

A calculated spectrum of fission neutrons is shown in Fig. 2-1 [1]. The energy deposited in the reactor core comes mainly from the fission fragments. A break down is given in Table 2-1.

Table 2-1: *Energy and range of reaction products in nuclear fission*

Reaction product	Energy (MeV)	Range in reactor core materials
fission fragmts.	167 ± 5	very short (< 1mm)
neutrons	5	medium (tens of cm)
prompt γ's	6 ± 1	long (10 cm ÷ some m)
β-particles	8 ± 1.5	short (mm to cm)
decay γ's	6 ± 1	long (10 cm ÷ some m)
neutrinos	12 ± 2.5	infinite
	204	

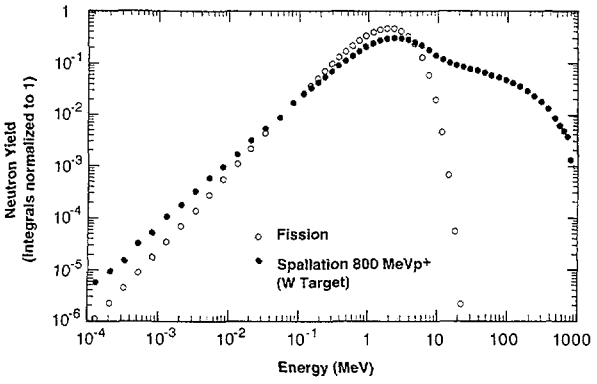

Figure 2-1:*Calculated neutron spectra for fission and for spallation in a Tungsten Target [1]*

2.2 The spallation process

The spallation process, in contrast to fission, is not an exothermal process: energetic particles are required to drive it and it can, therefore, be triggered in any nucleus, yet the neutron yield increases with the mass of the target nucleus. Although spallation is, of course also possible in uranium and yields about twice as many neutrons than in the heavy metals below the α-gap, we will limit

our discussions mainly to the latter, because the significant fission fraction in uranium complicates the issues on the one hand and Uranium targets do not play a role in high power research spallation sources because of metallurgical problems on the other.

The particles most commonly used to drive spallation reactions are protons of energies around 1 GeV. We will restrict our considerations mainly to this case. At this energy the de Broglie wavelength of the proton, $\lambda = h / \sqrt{2mE}$ is only of the order of 10^{-14} cm, which is significantly smaller than the diameter of a heavy nucleus. This is the justification for treating the interaction with the nucleus by the so-called cascade model, i.e. a series of collisions with individual nucleons inside the nucleus. A certain fraction of the incoming particle's kinetic energy is transferred to the nucleus by nucleon-nucleon collisions, thus increasing the kinetic energy of the nucleons, or, in other words, heating up the nucleus. According to the times involved, three stages can be distinguished in the spallation reaction:

In the initial *cascade*, which takes place within 10^{-22} seconds (the time it takes the incident proton to cross the nucleus), energy is transferred from the primary particle to individual nucleons inside the nucleus. In this process energetic particles may leave the nucleus and can induce another spallation reaction in a different nucleus. This is referred to as the *inter*-nuclear cascade, as opposed to the intra-nuclear cascade described above. The *intra*-nuclear cascade is often called "hadron cascade", since it involves charged pions, neutrons and protons. Following an intra-nuclear cascade the energy originally transferred to a few nucleons spreads more or less evenly throughout the nucleus via secondary ternary etc. collisions. This process occurs within 10^{-18} seconds or less and is called the transition stage, during which individual nucleons may occasionally be ejected from the nucleus. At its end the nucleus is in a highly excited state and, again, a Maxwell temperature can be attributed to it, which is, in general, somewhat higher than those of the fission fragments mentioned above. The following stage is nuclear evaporation which, like in the fission case, can be treated with the statistical mode.

2.3 Spallation neutron spectral and angular distribution

Careful analysis of neutron spectra measured for different target dimensions have shown that the energy distribution can indeed be described by three components:

$$n(E) = A_1 \cdot E^{1/2} \cdot \exp\left(-E / E_{T_1}\right) + A_2 \cdot E \cdot \exp\left(-E / E_{T_2}\right) + A_3 \cdot E \cdot \exp\left(-E / E_{T_3}\right) \quad (2.3)$$

with characteristic energies E_{T_i} that are attributed to the evaporation stage, the transition stage and the cascade stage respectively. About 90% of all emitted neutrons were found to belong to the evaporation and transition terms, with the characteristic energies E_{T_1} and E_{T_2} depending only little on the type of projectile but markedly on the size of the target (Tab. 2-2). This shows that significant "moderation" takes place, as the neutrons traverse a thick spallation target, either by "elastic" collisions or by secondary reactions at energies lower than that of the original proton.

The cascade part of the spectrum can, in particular for thin targets, reach up to the energy of the incident particle. It is strongly anisotropic with the higher energies emerging mainly in forward direction, as would be expected from collision kinetics.

Table 2-2: *Characteristic energy (MeV) of the evaporation part of the neutron spectrum from lead targets (from [3])*

Projectile	Thin target	Target 8x8x8 cm³	Target 20 ∅ x 60 cm³
Proton, 2 GeV	2.06 ± 0.08	1.70 ± 0.09	1.08 ± 0.04
Deuterons, 2GeV	2.06 ± 0.10	1.30 ± 0.06	1.00 ± 0.05

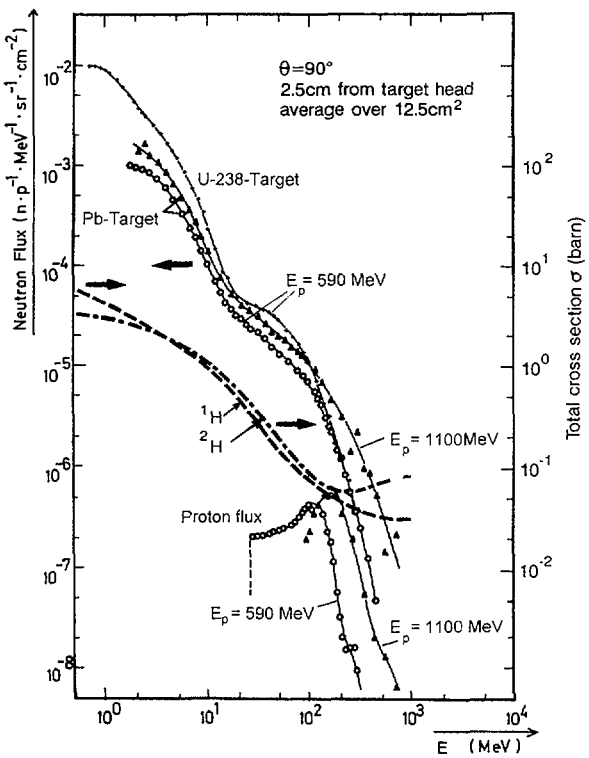

Figure 2-2: *Measured particle spectra from Lead and Uranium Targets for 590 and 1100 MeV proton beams.(after [2]). Also shown are the cross sections of H and D in the relevant energy range (right hand scale)*

Fig. 2-2 (after [2]) shows measured neutron spectra from thick targets at different energies and at 90° relative to the proton beam. An example for the angular distribution of the different energy groups is shown in Fig. 2-3 [3]. It should be noted that the average energy of all neutrons emitted ($\int E \cdot n(E)\, dE / \int n(E)\, dE$) is significantly higher than what would be calculated from the values of Tab. 2-2 with eqn. (2.2), because of the high leverage of the cascade neutrons whose energy is up to three orders of magnitude higher. For example, for the 20 cm diameter lead target the average energies at 30, 90 and 150 degrees relative to the 2.55 GeV proton beam were found to be 21.6, 7.31 and 4.38 MeV respectively. While this has important consequences on the shielding, on the one hand (cf. Ch. 6.2), it also opens up to take advantage of this anisotropy on the other.

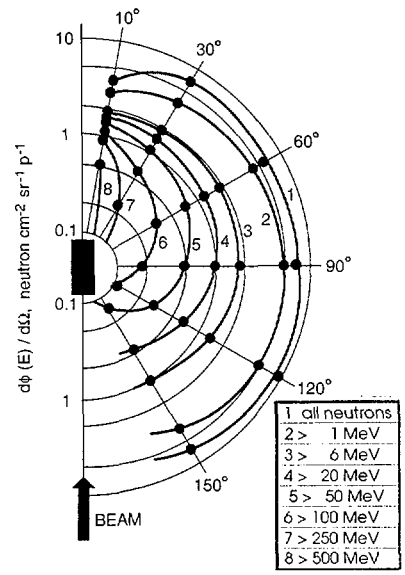

Figure 2-3: *Measured angular distribution of neutrons in different energy groups for a 20 cm diameter Lead target bombarded by protons of 2 GeV [3]*

In summary: about 90% of all neutrons released from thick targets in a spallation reaction can be described by characteristic energies around 1÷2 MeV and are emitted more or less isotropically. Their spectral and angular distributions thus resemble closely to those of fission neutrons (c.f. Fig. 2-1). The small fraction of cascade neutrons whose energy can reach up to that of the primary particles driving the reaction are emitted mainly in the forward hemisphere relative to the proton beam. As we will see later, they are difficult to moderate and thus constitute the main problem in shielding and activation in a spallation neutron source.

2.4 Power dissipation in spallation targets

It was mentioned earlier that the energy deposition in the target per spallation neutron is much lower than in a fission reactor core. A breakdown of the different contributions to this energy deposition is given in Table 2.3. Although these are calculated data for the special case of a slab-type water cooled lead target, they may be considered as more or less typical for spallation in any thick lead target. As can be seen, about 60% of the total energy of the incident 1 GeV proton are dissipated in the

target, most of it (except for the last two contributions) in the immediate vicinity of the nuclei that have been destroyed. Thus, since about 20 neutrons are generated by one 1.1 GeV proton (see below), the energy deposition per neutron in the target is little under 30 MeV. This compares to effectively 200 MeV per neutron in a fission core, because, out of the 2.4 neutrons generated per fission process, only 1 can contribute to the buildup of flux around the core, since the rest is needed to maintain the chain reaction or is lost by "parasitic" absorption.

Table 2-3:*Contributions from various particle types to energy deposition in the SNQ target (slab, 76.5% Pb, 7% Al, 16.5% D_2O) by 1.1 GeV protons. (The balance is mostly kinetic and binding energy of the neutrons.)*

	Energy Deposition	
Particle Type	MeV/ proton	percent
Primary Protons	213	37
Secondary Protons	233	41
Charged Pions	17	3
Neutral Pions	44	8
Muons	4	1
"Heavy" Particles[a]	17	3
Spallation γ-rays	14	2
Low-Energy Neutrons[b]	29	5
	571	100

[a] From recoil nuclei and heavy products (deuterons, tritons, ^{3}He, and alpha particles) evaporation

[b] From neutrons produced $\leq$ 15 MeV, and the secondary γ-rays they create

2.5 Spatial distribution of neutron generation and power deposition

It is important to note that, while the power distribution in a fission core can be controlled by the distribution of fuel, moderator and absorber, it can be influenced only very little in a spallation target:

In radial direction the power distribution is determined essentially by the intensity profile of the incoming beam, which widens somewhat as it travels down the length of the target. As we shall see later, while this distribution can, in principle, be influenced in the beam line, the options are very limited because what would be desirable for power density reasons, namely a flat profile, is difficult for the beam window because of thermal stress.

Axially, the distribution of the reactions in the target is essentially controlled by the cross section for nuclear interactions, which can be represented as

$$\sigma_{inel} = 15.9\pi \cdot A^{2/3} \quad mb / nucleus \qquad (2.4)$$

with A being the atomic number of the nucleus struck by a proton of energy above $\approx$ 50 MeV. This cross section is dominating at proton energies from a few hundred MeV to a few GeV. Outside this energy range other, competing processes play an increasing role, namely ionization losses below 100 MeV and pair production and other effects at the high energy end. As a consequence of this cross section, the intensity of the proton beam will decrease exponentially along the axis of the target, and so will the power deposition and the neutron release. A buildup zone is usually observed at the target head due to the internuclear cascade, which becomes more pronounced at higher energies. A reasonable parameterization of the axial distribution is obtained by the formula

$$n(z) = N_0\left(1-\exp\left(\frac{-z-z_0}{\lambda_b}\right)\right)\cdot\exp\left(-z/\lambda_a\right) \qquad (2.5)$$

where n, N_0 have the dimensions of the quantity to be described (neutron yield, power density, temperature, radial power integral) and the parameters can be attributed the following meaning)

z_0 extrapolation length (distance in front of the target at which the curve would cross zero

λ_b buildup length

λ_a attenuation length (essentially N_a/σ_{inel} where N_a is the number of target nuclei per cm^3). Typical values of λ_a are of the order of 10 - 20 cm for common spallation materials

These parameters do not have universal character. Especially when used to describe

the neutron leakage distribution on the surface, they depend on the target geometry and neutron energy range under consideration. If they are known however, eq. (2.5) is useful for analytical considerations.

2.6 Spallation neutron yield

One of the most interesting quantities for practical purposes is the number of neutrons obtained per proton. Again, this integral value depends not only on the material but also on the size of the target because of the internuclear cascade. The results of early measurement of the neutron yield Y(E) carried out on targets of 10 cm diameter and 60 cm length with proton energy between 200 MeV and 1.5 GeV were parameterized as

$$Y(E) = a(A+20)\,(E_{GeV} - b) \quad (0.2 \leq 1.5\ \text{GeV}) \quad (2.6)$$

where A is the atomic mass of the nucleus and $b \approx 0.12$ GeV. Although not physically correct, this can be considered like a "threshold" below which spallation becomes very improbable in competition with energy losses by ionization. The value a is 0.1 for all heavy elements except for 238-U, where it is 0.19. Thus, spallation in 238-U yields nearly twice as many neutrons per proton than in other heavy metals.

For a more extended range of incident energies the above linear correlation is no more correct. Vassil'kov et al have analyzed neutron yields up to 7 GeV of incident energies and for different projectiles on a 20 cm diameter target of Pb (Fig. 2-4, [4]). They derived the relation

$$Y(E) = -8.2 + 29.3\,(E_{GeV})^{0.75} \quad (2.7)$$

for protons on lead. In Fig. 2.4 the dashed and dotted lines give the results of eqns. (2.6) and (2.7). Recently, measurements of the neutron multiplicities [5] have yielded deeper insights into the physics of the spallation reaction but have, in general confirmed the older more integral measurements.

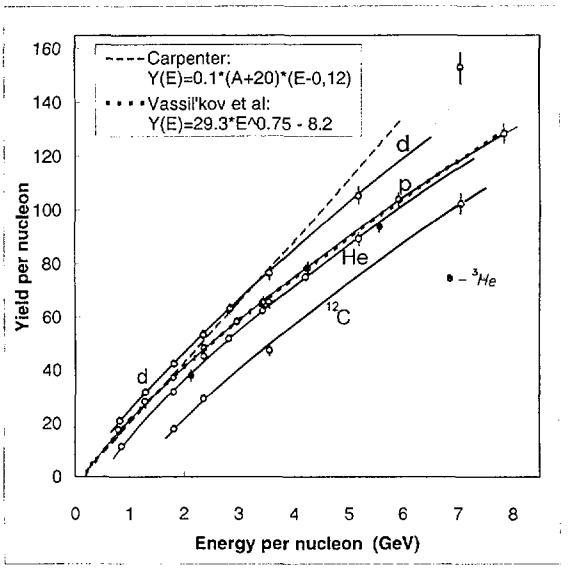

Figure 2-4: *Measured neuron yield from thick lead targets as a function of particle energy for different types of projectiles [Vas91]. The dashed line represents eqn. (2.6) and the dotted one eqn. (2.7) for protons.*

2.7 Spallation products

During the spallation process not only neutrons but also protons (cf. Fig. 2.2) and other light nuclei (^{2}H, ^{3}H, He) are emitted from the excited nuclei. As a consequence, the residual nuclei are not only neutron-poor isotopes of the parent nucleus that decay (mainly by internal $p \rightarrow n$ conversion and β^{+} emission) into lower Z elements, but these lighter elements are also created directly in the spallation process. Furthermore, there is always a certain probability for a highly excited nucleus to fission and therefore one also finds medium-heavy and light nuclei in the spectrum of spallation products even for classically "non-fissionable" materials. Finally, capture reactions can even lead to heavier nuclei than the parent nucleus which, in particular for the cases of Pb and Bi leads to generation of small amounts of Po. Fig. 2.5 shows the calculated distribution of spallation products for PbBi [6].

It can be seen that, although in small quantities, most elements of the periodic table are generated in a heavy spallation target. The consequences this has on materials properties and possible reactions is not yet well explored (cf. Ch. 6).

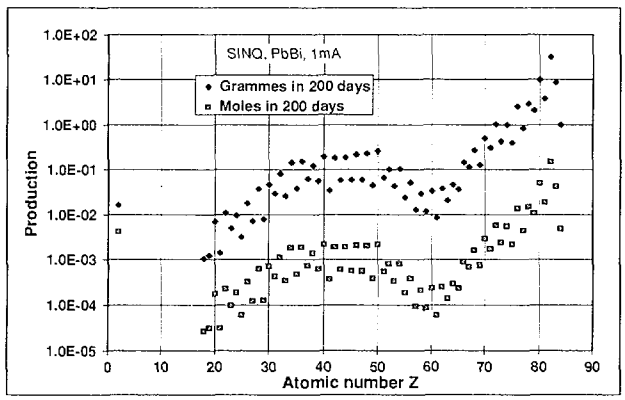

Figure 2-5:*Calculated distribution of reaction products in a Pb-Bi target after 200 days of irradiation with 1 mA of protons in a thermal neutron environment.*

3. Slowing down of fast neutrons in matter

Although Monte Carlo methods are now widely used to study complex target-moderator-reflector assemblies as a unit, we briefly review, in a cursory way, the mechanisms and processed involved in neutron moderation in order to illustrate the design options that exist in devising moderators that meet the goals of different types of neutron sources.

Neutron moderation occurs by "elastic" collisions of neutrons with the atoms of the moderator material. In each collision during the slowing down process the neutron transfers, on average, a certain fraction of its kinetic energy to the atoms of the moderator, i.e. E_1/E_2 is a constant. The logarithm of this constant, $\xi = \ln E_1 - \ln E_2$ is called the logarithmic energy decrement and is given by

$$\xi = \ln E_1 - \ln E_2 = 1-(\alpha_0\varepsilon/(1-\alpha_0\varepsilon)). \qquad (3.1)$$

$\xi = 1$ for A=1 and $\approx 2/(A+2/3)$ for A >1

with $\varepsilon = \ln(1/\alpha_0)$ and $\alpha_0 = (A-1)^2/(A+1)^2$

A is the atomic number of the moderator atom. This immediately shows that hydrogen is the most efficient element in terms of neutron moderation. The number of collisions, x, required to slow down a neutron from its original energy E_0 to an energy E_f is then given by

$$x = 1/\xi * \ln(E_0/E_f) \qquad (3.2)$$

Values of ξ and x (for E_0 = 2 MeV and E_f = 1 eV) are listed in Table 3-1, together with other quantities relevant for neutron slowing-down in selected elements and compounds.

The values of the free atom scattering cross sections σ_{fr} given in Table 3-1 are more or less constant over a large energy range for most elements, as long as the neutron energy is higher than, or of the order of, the binding energy of the atoms in molecules or condensed matter. This is the case down to around 1eV. As an example the scattering cross section of hydrogen is given in Fig. 3-1.

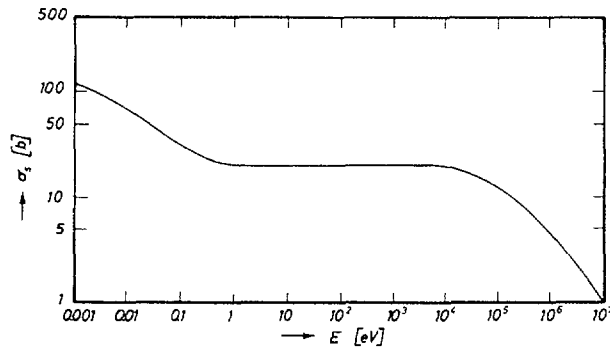

Figure 3-1:*The scattering cross section of hydrogen as a function of the energy of the incident neutron*

The probability of a collision to happen depends on the macroscopic cross section

$$\Sigma = \sigma/N = 1/\Lambda \qquad (3.3)$$

with σ being the microscopic cross section and N the number of atoms per unit volume. Λ is the mean free path between collisions. Λ being constant, the time t_i between collisions, and therefore the number of neutrons present in a certain velocity interval, is inversely proportional to the neutron velocity, v_i.

$$t_i = \Lambda/v_i = 1/(\Sigma_{fr} * v_i) \text{ or } t_i * v_i = \Lambda \approx \text{const.} \qquad (3.4)$$

Because the neutron flux can be interpreted as the product of the number of neutrons per unit volume in a certain velocity interval times their velocity, the neutron flux in the slowing-down regime depends on the neutron velocity as v^{-2} or as E^{-1}. In small moderators

this law will be modified. A convenient representation of the neutron current from the moderator surface reads [7]

$$\langle I(E)_{sd}\rangle = I(E_r)*(E_r/E)^{(1-\alpha)} \qquad (3.5)$$
$$= [E*I(E)]_{Er}*(1/E)*(E/E_r)^{\alpha}$$

with E_r being a reference energy (usually 1eV) and α depending on absorption in and leakage from the moderator during the slowing-down process. For non-reflected small moderators α is of the order of 0.2, but can be significantly reduced, depending on the moderator environment. $[E*I(E)]_{Eo}$ is frequently referred to as "epithermal flux" Φ_{epi}.

Equ. (3.4) also suggests that the total time it takes to slow a neutron down to a final velocity v is inversely proportional to v. A more rigorous theory [7] yields for the time dependence of the slowing down flux after a short source pulse a function of the product v*t only:

$$\Phi(v,t) \sim (\xi\Sigma_{fr}vt/\gamma)^{2/\gamma} \exp(-\xi\Sigma_{fr}vt/\gamma) \qquad (3.6)$$

with $\gamma = 1$ for A=1 and $\approx 4/(3A)$ for A>1. (3.7)

The average slowing-down time t_s, its standard deviation Δt_s and the FWHM $\Delta t_{1/2}$ are then found as:

$$v*t_s = (1+2/\gamma)*\gamma/(\xi*\Sigma_{fr}) \qquad (3.8)$$

$$v*\Delta t_s = (1+2/\gamma)^{1/2}\gamma/(\xi*\Sigma_{fr}) \qquad (3.9)$$

$$v*\Delta t_{1/2} = 3/(\xi*\Sigma_{fr}) \qquad (3.10)$$

t_s gives the delay between when the peak of the velocity distribution reaches v in the moderator (t_0 for the time of flight measurement) relative to when the proton pulse was injected into the target, whereas Δt_s and $\Delta t_{1/2}$ represent the standard deviation and the full width at half maximum of the pulse. Numerical values for these quantities are included in Table 3-1 for some elements and for compounds with high hydrogen content. In cases where the substances are gaseous at room temperature, values corresponding to the liquid at its boiling temperature are given. The quantities ξ and γ were computed using the formulae given in [7] rather than the approximations of equs. (3.1) and (3.7), but differences are minor even for the light elements. Averaging for compounds was done by weighting by the free atom cross sections σ_{fr}.

Clearly materials to be used in an optimized moderator-reflector system depend on the design goals to be met:

- Since the mean free path between collisions is essentially determined by $\Lambda = 1/\Sigma_{fr}$, in order to avoid excessive spreading of the neutrons, a large value of Σ_{fr} is desirable in most cases.
- In order to build up a high time average flux, a long life time of the neutrons in the moderator, and hence a small value of σ_a is important.
- If a high fast flux shall be maintained, a small value of ξ is desirable, whereas ξ should be high to achieve good time structure of the pulse and a small fast neutron background in thermal and cold spectra.

In cases where different materials are used for the moderator and the reflector, the moderator should have a large value of ξ, whereas for a good reflector ξ should be small in order to return as many neutrons as possible to the moderator without significant energy loss to make for a short pulse length.

As an illustration, we show in Fig. 3-2 results of a simple 1-D diffusion calculation for a source in a 20 cm diameter sphere inside a large volume of different materials. [9]. The left frame shows the spatial distribution of the slowing-down flux when it reaches 25 meV, whereas the flux distribution in thermal equilibrium is shown in the right frame. In all cases neutron absorption in the source has been neglected to illustrate the characteristics of the moderator. This means that the flux depression, which usually occurs in the vicinity of an absorbing target and whose magnitude depends on the properties of the moderator as well is not present. If fast neutrons are fed from the source continuously both, the slowing-down and the storage component (which represents the thermal equilibrium of the neutrons with the moderator), will always be present in the moderator. If only a short pulse is injected, the transient component

will prevail during the time Δt_s , which, for H_20 and v = 2000 m/sec (thermal neutrons) is little more than 5 μsec. During that time the storage component builds up and afterwards absorption and leakage through the surface will determine the decay of the flux in the moderator. Once again, this is a highly simplified visualization of what is going on, but is helpful for a general understanding.

Table 3-1: *Quantities relevant for neutron slowing down for a few elements and hydrogen rich compounds*

Parameter	Element									
	H	D	Be	C	N	O	Fe	Ni	Hg	Pb
A	1	2	9,01	12,01	14	16	55,85	58,71	200,6	207,19
σ_{tr} (10^{-24} cm^2)	20,51	3,40	6,18	4,73	10,03	3,75	11,21	17,89	26,53	11,01
σ_b (10^{-24} cm^2)	82,02	7,64	7,63	5,551	11,51	4,232	11,62	18,5	26,8	11,118
σ_{inc}	80,27	2,05	0,0018	0,001	0,5	0,008	0,4	5,2	6,6	0,003
σ_a (10^{-24} cm^2)	0,3326	0,0005	0,0076	0,0035	1,9	0,0002	2,56	4,49	372,3	0,171
ρ (g/cm^3) (*)	0,07	0,163	1,85	2,3	0,804	1,13	7,9	8,9	13,55	11,3
N (10^{24}/cm^3)	0,042	0,049	0,124	0,115	0,035	0,043	0,085	0,091	0,041	0,033
$\Sigma_{tr} = N^*\sigma_{tr}$ (cm^{-1})	0,86	0,17	0,76	0,55	0,35	0,16	0,96	1,63	1,08	0,36
ξ	1,000	0,725	0,206	0,158	0,136	0,120	0,035	0,034	0,010	0,010
γ	1,000	0,584	0,143	0,108	0,093	0,082	0,024	0,023	0,007	0,006
x (2MeV→1eV)	14,5	20,0	70,3	92,0	106,5	121,0	410,0	430,8	1460,1	1507,9
v^*t_s (cm)	3,47	21,37	13,58	24,51	44,28	108,83	59,86	36,77	187,06	576,49
$v^*\Delta t_s$ (cm)	1,74	10,69	6,79	12,25	22,14	54,42	29,93	18,39	93,53	288,24
$v^*\Delta t_{1/2}$ (cm)	3,47	24,81	19,01	34,88	63,47	156,85	88,73	54,54	279,66	861,96

Table 3-1 *(continued)*

Parameter	Compound					
	H_2O	CH_4	$(CH_2)_n$	NH_3	TiH_2	D_20
A	18	16	14	17	49,92	20
σ_{tr} (10^{-24} cm^2)	44,8	86,8	45,7	71,5	42,43	10,5
σ_b (10^{-24} cm^2)	168,3	333,6	169,6	257,6	163,3	19,5
σ_{inc}	160,5	321,1	160,5	241,3	165,5	4,1
σ_a (10^{-24} cm^2)	0,665	1,334	0,669	2,898	6,755	0,001
ρ (g/cm^3) (*)	1	0,453	0,94	0,682	3,978	1,1
N (10^{24}/cm^3)	0,033	0,017	0,040	0,024	0,048	0,033
$\Sigma_{tr} = N^*\sigma_{tr}$ (cm^{-1})	1,50	1,48	1,85	1,73	2,04	0,35
ξ	0,926	0,954	0,913	0,879	0,968	0,510
γ	0,923	0,951	0,908	0,873	0,967	0,405
x (2MeV→1eV)	15,7	15,2	15,9	16,5	15,0	28,4
v^*t_s (cm)	2,11	2,09	1,72	1,89	1,505	13,51
$v^*\Delta t_s$ (cm)	1,054	1,046	0,861	0,945	0,753	6,754
$v^*\Delta t_{1/2}$ (cm)	2,16	2,13	1,78	1,97	1,52	16,85

(*) σ_a is for thermal neutrons (2200 m/s); cross section data are from ref [10]; for H, D, N, O,CH_4 and NH_3 ρ is given at the respective boiling points at 1 atm; for the compounds cross sections and N are given per molecule

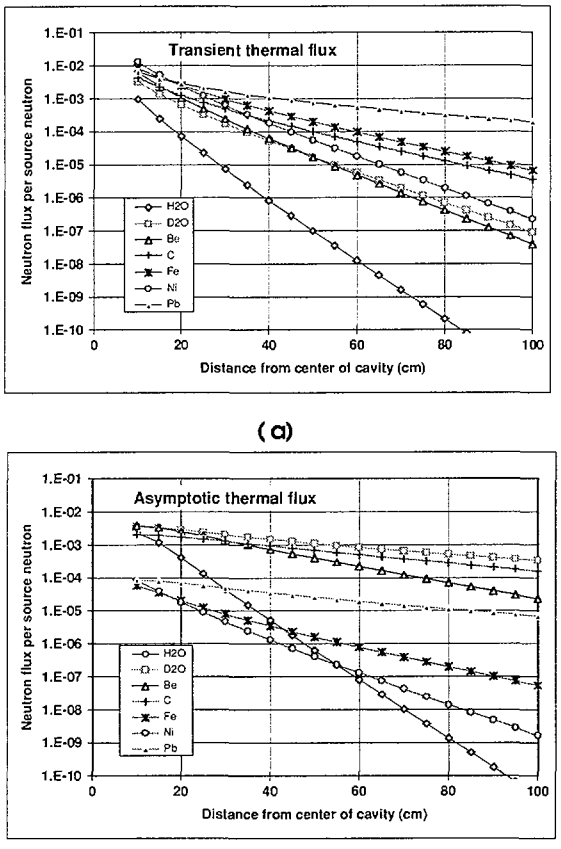

Figure 3-2: *Distribution of slowing down flux ("transient flux", top) and thermal equilibrium flux ("asymptotic flux", bottom) in 1D diffusion approximation for different moderator materials with an absorption-free fast neutron source of 2 MeV in a 10 cm radius cavity.*

It is obvious from the data in Table 3-1 and Fig. 3-2 that, as an element, hydrogen is by far the best moderator. In order to have a high enough density, it must be either in the liquid (or supercritical) state, or a compound with high hydrogen content must be used. If any of the hydrogen-rich compounds can be used, for which $v^*\Delta t_s$ is $\approx$1cm, this makes a better moderator than liquid hydrogen with $v^*\Delta t_s$ = 1.74 cm.

Although the approximation of a constant scattering cross section is valid only above about 1 eV, the slowing-down regime extends to an energy corresponding to roughly 5 times the effective moderator temperature, T_{eff}, because moderation continues until equilibrium with the thermal motion of the moderator atoms is reached. Below this limit an energy distribution of the neutrons is observed, which represents more or less thermal equilibrium between the moderator atoms and the neutrons. It is described by the Maxwellian distribution:

$$\Phi(E)_M = \Phi_{th}\, E/(k_B T_{eff})^2 \exp\,(-E/(k_B T_{eff})) \qquad (3.11)$$

where Φ_{th} is the thermal neutron flux and k_B = 0,08866165 meV/K is Boltzman's constant. The transition between the slowing-down regime and the thermal equilibrium spectrum which at about $5kT_{eff}$ is usually taken into account by a switch function $\Delta_1(E)$, by which the slowing down spectrum is multiplied. A frequently used formula is

$$\Delta_1 = 1/(1+5\, k_B T_{eff})^5 \qquad (3.12)$$

The full representation of the spectrum, including equ. (3.5) then reads:

$$\Phi(E) = \Phi_{epi}{}^*(1/E)^*(E/E_r)^{\alpha}\, \Delta_1(E) + \Phi_{th}\, E/(k_B T_{eff})^2 \exp\,(-E/k_B T_{eff}) \qquad (3.13)$$

Note that, while Φ_{th} is an energy integral Φ_{epi} is not. Φ_{epi} corresponds to what is called flux per unit lethargy $\Phi(u)$ in reactor terms, with $u = \ln(E_0/E)$.

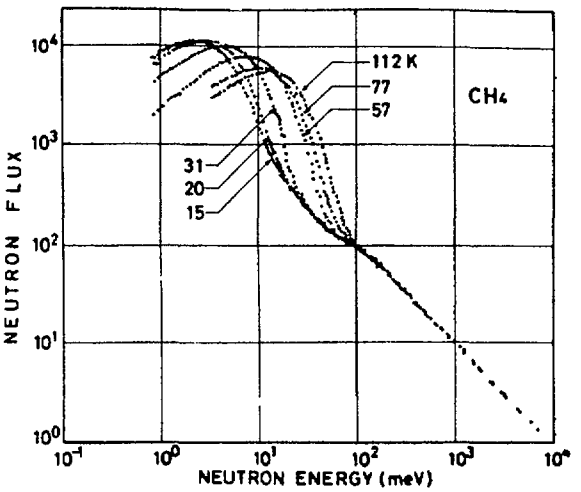

Figure 3-3: *Energy spectra from a solid methane moderator at various temperatures [11].*

An example for a moderator at different temperatures is shown in Fig. 3-3. While in the slowing down regime above 100 meV the flux is independent of the moderator temperature and proportional to 1/E, the Maxwellian part shifts to lower energies as the temperature is decreased. The deviation from the 1/E behavior below 100 meV for low temperatures may be attributed to the increase in scattering cross section and

hence a shorter life time of the neutrons at the respective energies during slowing down.

Note: *There is a strong incentive to use cryogenic moderators in research neutron sources in order to shift the Maxwellian distribution to lower energies. This has two consequences, as can be seen from Fig.3-3:*

(1) it increases the phase space density of the slow neutrons, which are of growing importance in the source utilization and

(2) it extends the slowing-down regime with its narrow pulses: The result $v^*\Delta t_s$ = const. (equ.3.9) is very important for pulsed research neutron sources for two reasons:

(a) It shows that, if neutrons from the slowing-down regime are used, the resolution of a time of flight instrument, which is inversely proportional to the neutron velocity, remains constant because the pulse width decreases as the velocity increases.
(b) *While the time-average flux of slowing-down neutrons on a pulsed source is not higher than on a continuous source, rather lower because of the faster moderators used, the instantaneous flux during the pulse is enhanced by a factor v on top of the compression into short pulses.*

The importance of cryogenic moderators and related design issues have recently been reviewed [8] and will not be treated here. An international R&D program is going on to develop more efficient cryogenic moderators than are presently available for high power pulsed neutron sources [10]

4. General design features of research spallation neutron sources

Research neutron sources are nowadays mainly designed for neutron scattering applications, for which spallation neutron sources can offer the extra advantage of a time structure that is almost ideally matched to certain experimental techniques. Being driven by an accelerated proton beam, spallation neutron sources can be built with almost any desired time structure on the fast neutron flux emerging from the target, provided there is not too much moderation in the target itself. Liquid metal targets, as they are now widely considered in the new medium to high power spallation sources fulfill this condition in an almost ideal way. Depending on the type of accelerator driving the source, three classes can be distinguished:

(a) *Continuous spallation sources*
For spallation neutron sources fed from an accelerator with no macro-time structure such as a cyclotron or a cw-linac the optimization goal naturally is a high time average flux. Use of low absorption materials in and around the target is crucial in order to ensure a long life time of moderated neutrons. The moderator should be large to achieve complete thermalization and minimum leakage losses. Typically, a 2m diameter D_2O tank will surround the target, acting as moderator and reflector at the same time. As can be seen from Table 3-1, D_2O has almost no neutron absorption. Its mean free path between collisions is rather large. As a consequence, there is a fairly large region of high thermal flux in the moderator (cf. Fig. 3-2 b), which allows to move the beam tube noses some distance away from the target and thus achieve a much lower fast and high energy neutron background than is usually found on pulsed spallation sources, where the moderators are placed as closely as possible to the target as technically feasible. Cold moderators in continuous sources will be of the rethemalizing type, i.e. they will be embedded in the surrounding D_2O and will shift the ambient temperature equilibrium spectrum to cryogenic temperatures. Therefore liquid D_2 is the preferred cold moderator material. This is the same situation as it exists in modern research reactors. The only existing source of this type is SINQ at the Paul Scherrer Institut in Switzerland (cf. ch. 5.1). It is the most powerful operational spallation neutron source in

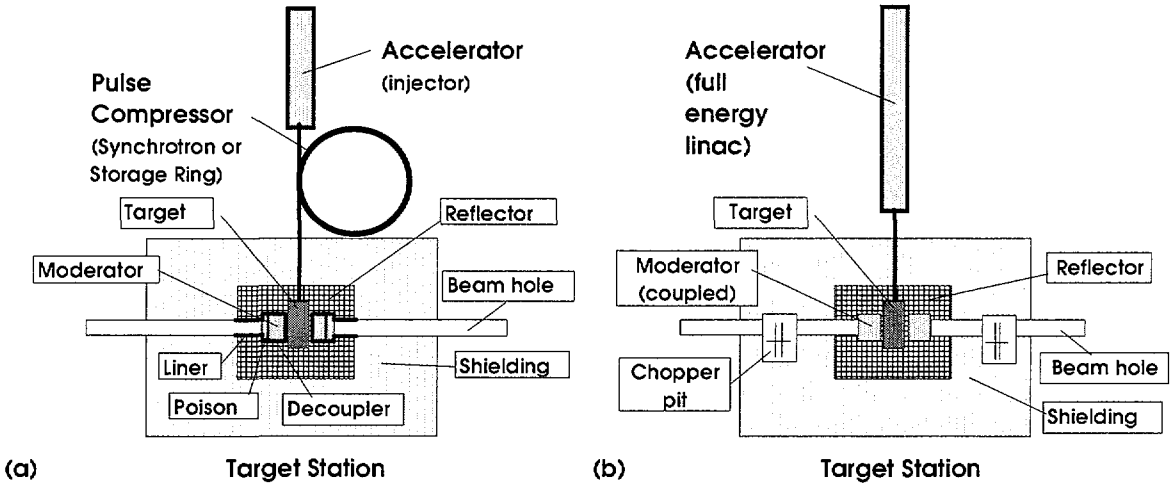

Figure 4-1 *Schematic representation of pulsed neutron source arrangements. (a) short pulse source with decoupled and poisoned moderator, requiring proton pulse compression (b) long pulse source with coupled moderator and with direct injection from the linac. In real configurations the moderators will be viewed by the beam tubes in a "tangential" way, i.e. such that the beam tube does not see the target through the moderator.*

the world, and will be described in some detail below, because it offers unique research opportunities in the field of high power spallation targets.

(b) Short pulse neutron sources

While continuous neutron sources favor those neutron applications that require a high time average flux, there is a whole class of neutron scattering techniques that work in a pulsed mode (time of flight experiments) and hence can be served best by a high peak flux at appropriate repetition rates. It is with those instruments in mind that short pulse spallation neutron sources were developed. Their characteristic feature is that they generate fast neutron pulses which are short enough so they don't contribute noticeably to the width of the moderated neutron pulse in the whole energy interval of interest. This requires single turn extraction of a stored beam from a ring that can either be a rapid cycling synchrotron, as in IPNS and ISIS or an accumulator/storage ring fed by a full energy linac as in MLNSC at Los Alamos (cf. Table 5-1). Both types are also being proposed in new projects. The optimization criterion in this type of source is a short pulse duration without disproportionate losses in peak flux. Rapid slowing down and a short neutron life time in the moderator after thermal equilibrium has been reached are at a premium. In order to accomplish the latter, moderators are often surrounded by neutron absorbing material (decouplers) to prevent slow neutrons from being returned from the reflector. Often absorbing material is even placed at a certain depth inside the moderator (Fig. 4-1a), in order to limit the time slow neutrons spend diffusing out of the moderator. This kind of arrangement has been designated "high resolution". Obviously, this is on the expense of intensity. Up to a factor of 10 or more can be gained by doing away with the decoupler and poison and using "coupled" moderators, where the extra pulse width can be tolerated from a resolution point of view. This type of moderator is referred to as "high intensity". For short proton pulses neutron pulses from both moderators have a steep rising edge and comparable (within a factor of 2) peak flux. The extra intensity for coupled moderators is primarily in the longer trailing edge.

(c) Long pulse spallation neutron sources

A spallation source fed directly from a

pulsed linac is usually referred to as a long pulse source, meaning that the pulse length of the proton beam is significantly longer than the time it takes to slow the neutrons down in the moderator. The pulse width of these sources is thus essentially determined by the duration of the proton pulse and will be of the order of 1 ms. Again, high time average flux is an important optimization criterion, but also the pulse shape becomes important, especially if chopper instruments for time of flight spectroscopy are to be used. Due to the short opening time of the chopper, which must be placed at a certain distance from the moderator (cf. Fig. 4-1b), slow neutrons that pass the chopper will have started at the moderator earlier than fast ones, which pass the chopper at the same time. The pulse shape therefore is convoluted into the spectral distribution of neutrons from the moderator in this technique. Precise knowledge of the intensity as a function of wavelength is, however, crucial in inverted time of flight experiments because data taken at different wavelengths must be compared to each other intensity wise. It is, therefore, important in this type of source to find the right compromise between high peak flux and neutron life time in the moderator [12],[13]. A flat top pulse shape is, therefore, desirable. For this reason the moderators, even cryogenic ones, will still be of the slowing-down type but no measures will be taken to artificially reduce the neutron life time, i.e. the moderators will be tightly coupled (Fig. 4-1b). A moderator design as used in continuous sources would distort the pulse shape too strongly due to the very long life time of the neutrons.

To a good approximation, the pulse shape in a pulsed source can be represented for all neutron energies by the relations

$$\Phi(t) = \Phi_{as}(1-\exp(-t/\tau) \qquad \text{for } t \le t_p$$

$$\Phi(t) = \Phi_{as}(1-\exp(-t_p/\tau)\exp(-(t-t_p)/\tau) \qquad \text{for } t \ge t_p \qquad (4.1)$$

with t_p being the duration of the proton pulse and τ the life time of the neutrons which depends on the neutron energy. Φ_{as} is the flux that would be reached if the beam was on at full intensity all the time. The average flux is $\Phi_{av} = \Phi_{as} \cdot t_p\nu$ with ν being the pulse repetition rate. Frequently more than one τ will be required to characterize a moderator in its environment. As an example, we show in Fig. 4-2 the pulse shape calculated for a room temperature coupled (high intensity) H_2O moderator with Lead reflector for the ESS-project. The original pulse was calculated by Monte Carlo techniques; the dashed curve was obtained, using a sum of terms as given in equ. (4.1) with three decay constants τ_i of 8, 65 and 180 μsec and relative respective weights of 0.373, 0.522 and 0.105. (Although not derived on physic grounds, the three decay constants may be visualised as representing the slowing-down part (transient flux in the moderator), the reflector return part (transient part in the reflector for epithermal neutrons) and the storage term in the moderator. For comparison, the pulse is also shown that would be obtained if the unchopped Linac pulse of 1 ms duration (with 66 % more protons in the pulse, cf. ch. 5.2) would be injected directly into the same moderator. (Short and long pulse modes).

While the first long pulse neutron source, SNQ [14], [15] was proposed almost two decades ago, no such facility has been realized so far. Recently, however, interest in long pulse sources is growing again, with particular emphasis on the use of slow neutrons (cold moderators) [16], [17] requiring a longer pulse duration than planned for SNQ. Technically a long pulse source is clearly simpler than a short pulse source. While different in its layout, its technical implications are more like those of a continuous source, in that it does not require a pulse compressing ring and does not suffer from the thermal shock one has to deal with in the targets of high power short pulse sources (cf. ch. 5.2).

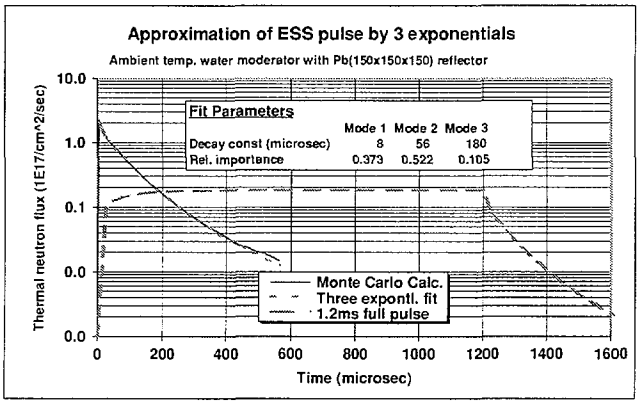

Figure 4.2: *Pulse shapes calculated for the ESS moderator-reflector configuration by Monte Carlo methods, and fit with three decay constants for a short pulse. Also shown is the pulse that would be obtained for direct injection of the 1.2 ms proton pulse from the linac containing 66% more protons, because unchopped.*

5. Specific examples of research spallation neutron sources

Although the first neutrons generated were from particle driven sources, fission reactors took over in the early 40ies with a spectacular increase in thermal neutron flux within a few years. The historic trend in flux development is shown in Fig. 5-1. For pulsed sources two values connected by a vertical line are shown, giving the peak and average flux. Clearly, for fission reactors the limits of present fuel technology have more or less been reached. On the spallation source side some more development can still be expected, because, not only is the heat release per neutron almost five times smaller than in a fission core, there are also more options to cope with the high power density, at least for long pulse and continuous sources.

Table 5-1 shows the main characteristics of recent spallation sources and new proposals. Earlier spallation sources shown in Fig. 5-1 were add-ons to existing accelerators and were clearly pioneering the technology. This is particularly true for KENS in Japan and IPNS in the USA.

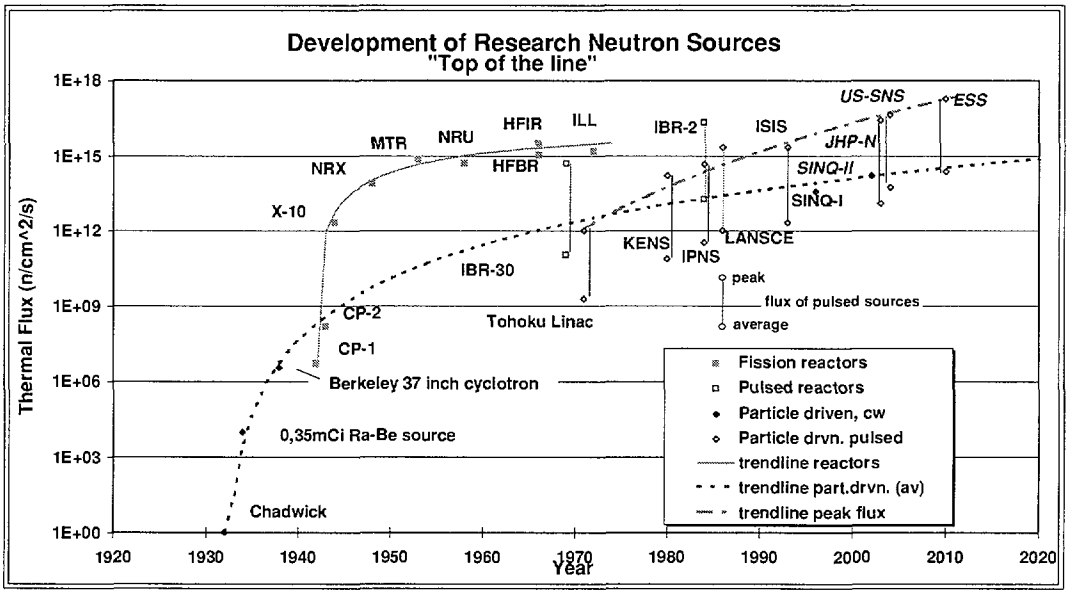

Figure 5-1 *The development of thermal neutron flux in different types of research neutron sources .For pulsed sources the peak and average flux is given, connected by a vertical line.*

As an illustration for the current frontiers in high power spallation sources, we will, in the following, give a brief description of the currently most powerful spallation source, the continuous source SINQ, and the most ambitious project presently under study in the field, the short pulsed neutron source ESS. Technological issues related to their optimization will be discussed in chapter 6.

Table 5-1: *Characteristics of recent and future research spallation neutron sources.*

Source and location	Type of accelerator	Proton energy (Gev)	Pulse frquency (Hz)	Time av. beam power (MW)	Type of target	Peak thermal flux* ($cm^{-2}s^{-1}$)	Time av. thermal flux* ($cm^{-2}s^{-1}$)	Status
ESS, EU	linac plus 2 compressors	1.33	50	5	liquid metal (Hg)	$2*10^{17}$	$2.5*10^{14}$	under study
SINQ, CH	cyclotron	0.57	con-tinuous	0.5	solid, Zy liqu., PbBi	$3.5\ 10^{13}$ $8.5\ 10^{13}$	$3.5\ 10^{13}$ $8.5\ 10^{13}$	operating in preparat.
ISIS, UK	synchrotron	0.8	50	0.16	solid, vol. cooled, Ta	$2.3x10^{15}$	$2x10^{12}$	operating
MLNSC, USA	linac plus PSR	0.8	20	0.08	solid, vol. cooled, W	$2.3x10^{15}$	$1x10^{12}$	operating
SNS, USA	linac plus compressor	1	50	1	liquid metal (Hg)	$4*10^{16}$	$6*10^{13}$	under design
AUSRTON Austria	synchrotron	1.6	10	0.4	solid, edge cooled W,	$3x10^{16}$	$5x10^{12}$	proposed
JHF-N 0.6 Japan	synchrotron	3	25	0.6	solid, vol. cooled, W	$1*10^{16}$	$8x10^{12}$	proposed
JNSC Japan	linac plus compressor	1.5	50	5	liqu. metal (Hg)	$2*10^{17}$	$2.5*10^{14}$	under study
MMF, RUS	linac (plus comp)	0.6		0.6	solid, vol, cooled W			commissio ning

** typical maximum values; precise figures vary, depending on type of moderator*

5.1 The Continuous spallation neutron source SINQ

5.1.1 The PSI accelerator complex

The accelerator complex of the Paul Scherrer Institut consists of four accelerators, three of which, the Cockroft-Walton pre-accelerator (870 keV), the Injector Cyclotron II (72 MeV) and the Main Ring Cyclotron (590 MeV) are forming a cascade to provide protons for a wide range of uses (Fig. 5-2). The fourth one, a commercial Phillips cyclotron (Injector I), was the original injector for the main ring and was replaced by a new one in the course of an upgrade program which took the current from its original design value of 100 μA through intermediate steps at 150 μA (the limit of Injector I) and 250 μA (the limit of the original rf-system on the main ring) to its present value of 1.5 mA. Currently Injector I supplies 72 MeV protons for isotope production, eye cancer treatment (OPTIS) and low energy nuclear experiments. It is also occasionally used to inject polarized protons of low current into the main ring. The high current beam extracted from the main ring at 99.8 % efficiency passes through a splitter region where about 20 μA are peeled off for use in the PIREX proton irradiation area, a nuclear physics experiment or for the newly installed isocentric gantry in which tumor treatment by

proton irradiation is being tested. The main part of the beam continues through two pion production targets, M ("mince", thin) and E ("épaix", thick), to produce pions and muons for a variety of applications in fundamental, nuclear and condensed matter physics. Although the assignment of the secondary beams from these targets is changed as required, it is now fair to say that about half of them are routinely used for condensed matter physics. This illustrates the wide use of an accelerator in fundamental and applied research.

Condensed matter physics and materials science are also the main scientific disciplines at the latest addition to the suite of proton beam driven devices at the PSI accelerator complex, the spallation neutron source SINQ.

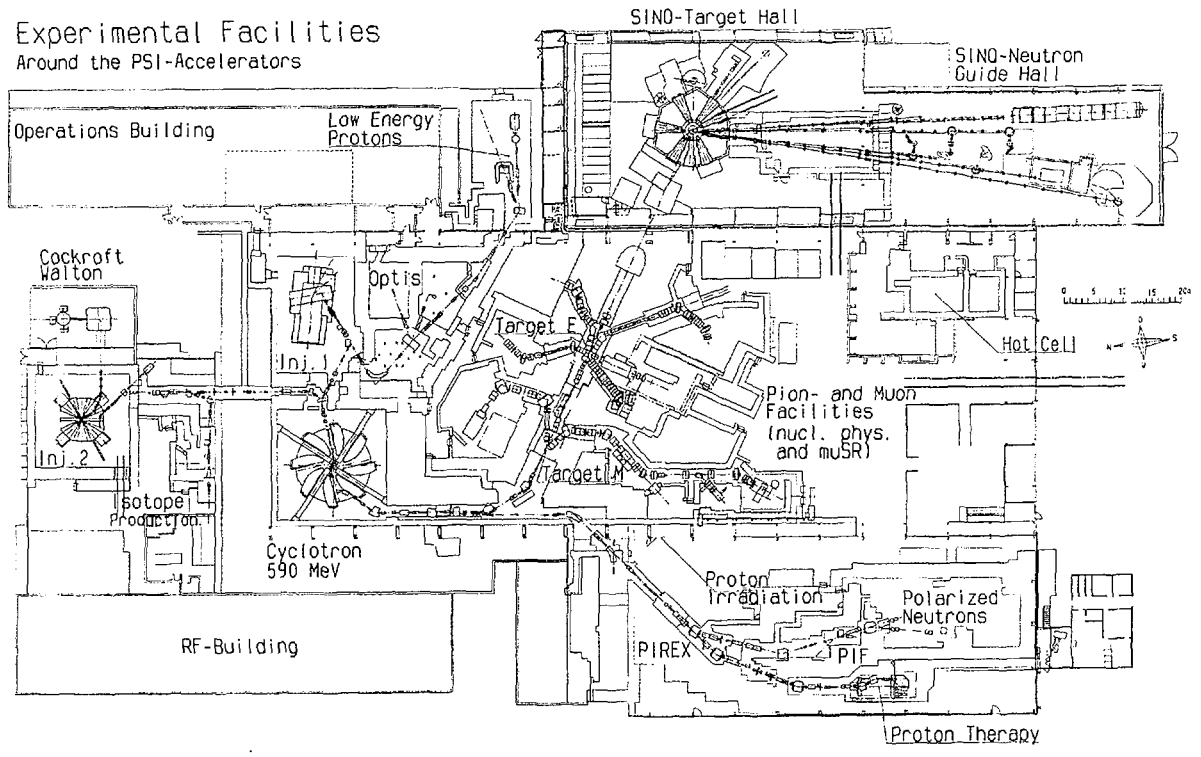

Figure 5-2: *Floor plan of the PSI accelerator complex and its experimental areas. Beyond target E the beam is bent downwards for transport to SINQ and vertical injection into the target from underneath.*

5.1.2. The SINQ Facility

When passing through target "E", a 6 cm thick graphite target, the proton beam loses about 20 MeV of energy and its momentum spread increases both longitudinally and transversely. In order to be able to transport the beam to the SINQ target at the desired low loss levels (for hands-on maintenance of most components) it must be reshaped by a set of collimators and slits. The net result is that, out of 1.5 mA hitting target E, 850 μA (57%) at 570 MeV can be transported to the SINQ target with a computed loss value of as little as 10 ppm on the last 25 m of beam line. This low loss was confirmed by measurement during the early commissioning phase of SINQ [18]. Because injection into the SINQ-target is from underneath (Fig. 5-3), the beam is bent downwards after target "E" to a level of -11 m and up again into the vertical direction. The arguments for this choice were a full 360° access to the target block circumference for beam extraction on the one hand and a plan to design a natural convection driven liquid metal target on the other [27]. While the former is still valid, the latter has gone away because cooling of the beam window is considered to require a more well defined flow configuration than can be guaranteed with natural convection alone.

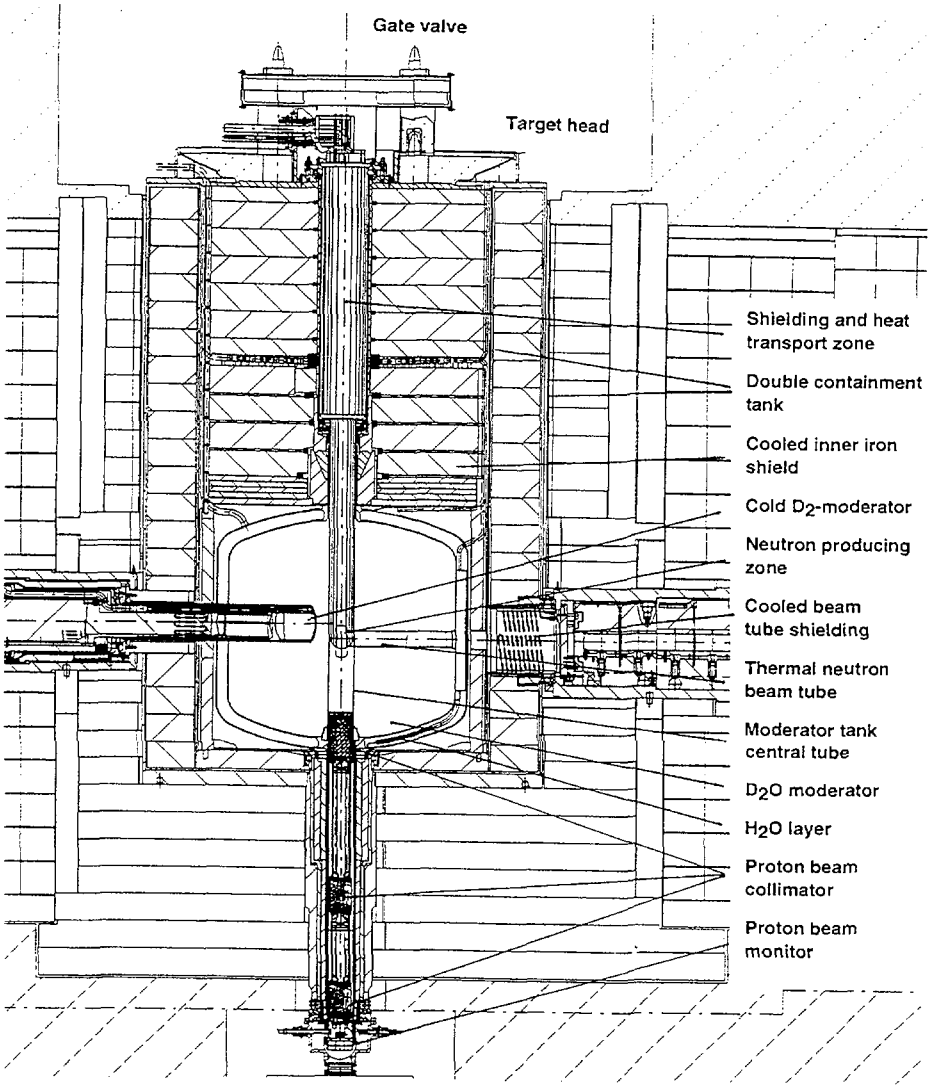

Figure 5-3 *The inner region of the SINQ target block with the beam collimator beneath the target and the cold D2 moderator and a beam port penetrating into the D2O moderator tank. The target is suspended from the heavy shielding above the moderator tank.*

Being driven by a cyclotron that delivers an essentially cw-beam (with an rf-bunch structure of 51 MHz), SINQ is optimized for high time average neutron flux by surrounding the target with a large (2 m diameter) D_2O-reflector and avoiding neutron absorption in the inner regions of SINQ to the largest possible extent. A well reflected volume of liquid D_2, at 25 K, serves to slow neutrons down below thermal energies and to supply "cold" neutrons for two beam tubes and seven supermirror coated neutron guides. Performance figures of the SINQ beams were reported elsewhere [19] and will not be repeated here. In summary, with its roughly 500 kW of beam power and its present Zircaloy target, SINQ performance is similar to that of a 10 MW MTR-type research reactor.

5.1.3 The SINQ target development program

In its current form the target (Fig. 5-4) is an array of D_2O-cooled Zircaloy-2 rods contained in a double walled Aluminum shell with separate D_2O cooling. Zircaloy was chosen as material for the startup and commissioning target because it is a well established and readily available material for nuclear applications and was found to yield nearly the same thermal flux in the reflector as the traditional spallation target materials

Tantalum or Tungsten because of its much lower neutron absorption [21]. As can be seen from Fig. 5-5, [22] other target alternatives, based on lead filled tubes of different materials would yield more flux, but the technology of such targets was not well enough established at the time when the first target was built. In the mean time, more research has been carried out along these lines theoretically [23], as well as experimentally [24], [25], which lead to inclusion of a few lead filled martensitic steel tubes into the present target as prototypic test elements.

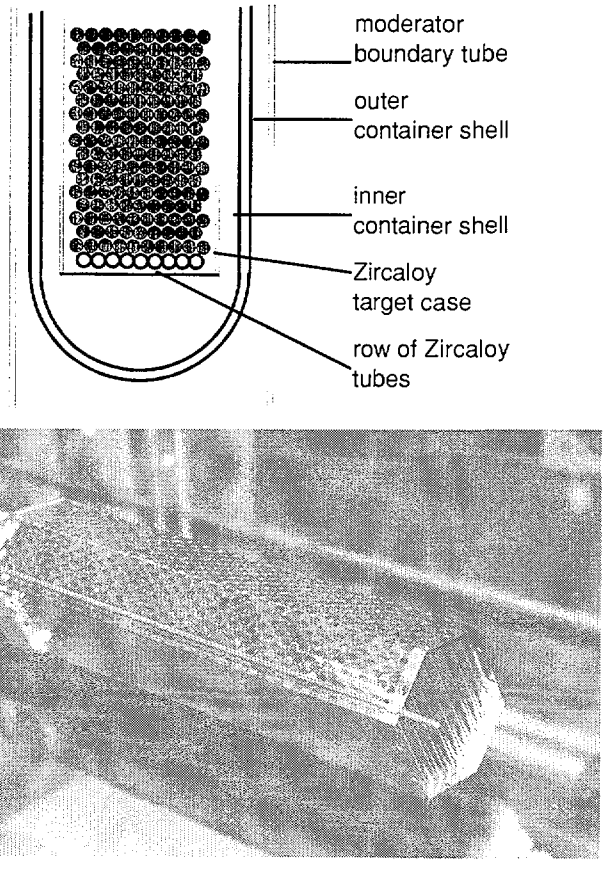

Figure 5-4: *The SINQ-rod target; schematic (top) and photograph of the rod bundle target (bottom)*

Even though a gain factor of about 1.6 in flux is expected from a steel clad lead rod target, there remains a strong incentive to move on to a liquid metal target in SINQ:

(1) another factor of 1.6 in flux over the lead filled steel tubes is expected from a liquid Lead-Bismuth eutectic target according to Monte Carlo calculations [22], if a 2 mm thick steel container is used.

(2) due to the fact that a liquid metal target contains no water in the reaction zone, not only is the proton beam converted into neutrons more efficiently, the absence of moderation inside the target pushes the flux maximum closer to the positions of the beam tube noses and production of radioactivity in the target water cooling loop will be almost completely eliminated, or at least significantly reduced.

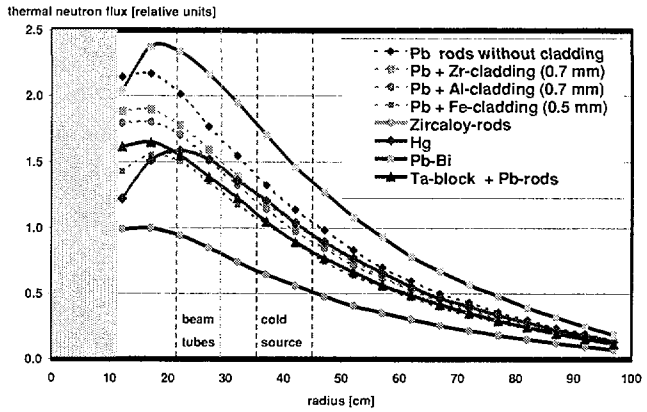

Figure 5-5: *Calculated flux in the reflector for different target options for SINQ. The positions of the beam tube noses and the cold moderators are at 25 and 40 cm from the target center line respectively*

Currently most of the radiation level in the SINQ cooling plant room stems from ^{7}Be, a spallation product of the oxygen in the cooling water and about 80-90% of the ^{7}Be produced is in the target cooling loop, which plates out almost quantitatively on the pipe work, leaving radiation levels virtually unchanged, when the water is drained from the loops [26].

Although a liquid metal target was on the agenda of the SINQ project from very early on [27], which is one of the reasons for the vertical target insertion, there are several questions to be resolved before such a concept can be licensed and used safely. Choice of the target material is one of them. There are several options that can be considered, as listed in Table 5-2. Of these, Lead has a rather high melting point, which makes its use difficult, because solidification must be avoided at all times and everywhere in the target. While it was found that a Mercury liquid metal target, despite its high thermal absorption cross section, would yield

roughly as high a flux level in the moderator as a steel clad lead rod target (Fig. 5-5), the option of a lead-bismuth target is the preferred one for SINQ, because it yields a significantly higher flux. Since there is no opportunity to drain the target prior to its removal from the target block, due to the beam injection from underneath, a material that can be solidified for the target transport seems to be a safer choice. The main question that needs to be resolved is the risk associated with the production of Polonium, an α-emitter, which is generated by thermal neutron capture in Bismuth as well as by (α,n)-reactions in Lead. In the SINQ environment the first process is by far the dominating one, making the Po-content in a PbBi-target about 1000 times higher than in a pure Pb-target. The R&D program for this target development has been described on several occasions [28], [29]. An outline will be given in Chapter 6, together with the one for the ESS target, since there are many common features, which pertain to any liquid metal target system.

Table 5-2: *Some relevant properties of possible liquid metal target candidate materials*

Property		Pb	Bi	LME *	LBE**	Hg
Composition		elem.	elem.	Pb 97.5% Mg 2.5%	Pb 45% Bi 55%	elem.
Atomic mass A (g/mole)		207.2	209	202.6	208.2	200.6
Density (g/cm^3)	20°C	11.35	9.75		10.5	
	liquid	10.7	10.07	10.6	10.5	13.55
Linear coefficient of thermal expansion ($10^{-5}\ K^{-1}$)	solid	2.91	1.75			
	liquid (400°C)	4		4		6.1
Volume change upon solidification (%)		3.32	-3.35	3.3	0	
Melting point (°C)		327.5	271.3	250	125	-38.87
Boiling point at 1 atm (°C)		1740	1560			356.58
Specific heat (J/gK)		0.14	0.15	0.15	0.15	0.12
Thermal neutron absorption (barn)		0.17	0.034	0.17	0.11	389

* LME - lead/magnesium eutectic ** LBE - lead/bismuth eutectic

5.2 The ESS project

5.2.1 the ESS concept and accelerator system

The European Spallation Neutron Source (ESS) is intended to become the next regional source in Europe, like the high flux reactor of the Institut Laue-Langevin has been for the past decades. When the basic specifications of ESS were decided (cf. Tab. 5-1), this was in full appreciation of the fact that a 5 MW beam power short pulse source would pose interesting challenges on the accelerator side as well as, and in particular, on the target side. After examining various options for the different components of the system, the study group formed in 1992 came up with a concept of a 1.33 GeV linac followed by two compressor rings. The two rings are foreseen because on theoretical grounds one expects a limit of about 2.10^{14} protons per ring due to space charge effects, whereas the average current of 3.75 mA at 50 Hz results in 4.63×10^{14} protons per pulse. The two rings are filled sequentially by chopping the 1.2 ms long pulse in the linac into 360 ns long micropulses with 240 ns long gaps between them (Fig. 5-6). With 1000 micropulses injected into one ring, a kicker magnet is activated during a 100 µsec long gap to direct the beam to the other ring. When both rings are full, extraction occurs over a single turn in each ring and the two 400 ns long subpulses are combined to a 1 µsec long double pulse to be transported to the target.

The need to have two compressor rings to provide the pulses necessary to meet the users' demands has a profound influence on the whole accelerator system. Without going

through the reasoning for the various choices, we give a brief description of the concept, as it resulted from the feasibility study [30]:

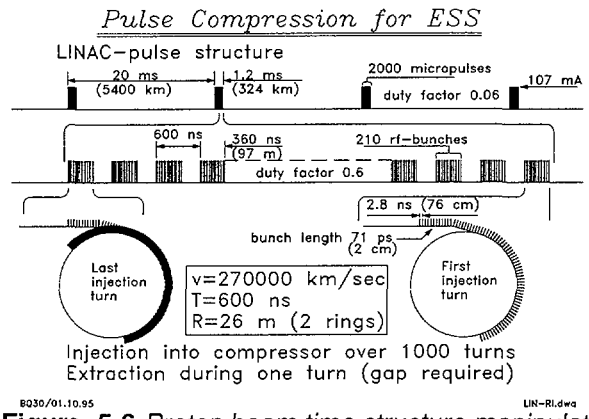

Figure. 5-6 *Proton beam time structure manipulation for injection into the ESS compressor rings.*

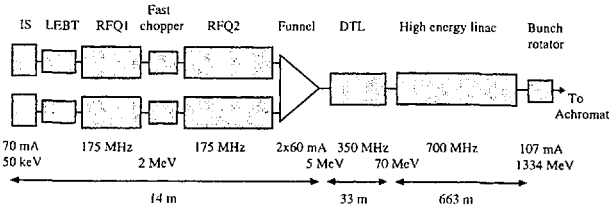

Figure 5-7 *Schematic of the ESS linac concept*

Because injection into the rings is by charge exchange, and there are no sufficiently powerful H^- sources available, two ion sources are required to produce the necessary current of 104 mA in the linac. Their beams will be combined in a funneling section at an energy of 5MeV, after pre-acceleration in two radiofrequency quadruopole (RFQ) structures, each with beam chopping to generate the micropulses. This results in doubling of the bunch frequency from 175 MHz in the RFQs to 350 MHz in the following drift tube linac (DTL), which accelerates the beam to 70 MeV. The bulk of the accelerating structure is a coupled cavity linac (CCL) with an rf-frequency of 700 MHz that takes the beam up to its final energy of 1334 MeV. The total length of the linac is little over 700 m with 663 m taken up by the CCL structure. Fig. 5-7 shows a schematic of the linac concept and Fig. 5-8 is an artist's view of the whole facility. All accelerator facilities (linac, 180° achromatic bend, compressor ring and beam transport line) are buried under concrete and dirt shielding. There are two target stations (high rep rate, 50 Hz and low rep rate, 10 Hz) which will share the proton pulses in a 4:1 ratio. Although ESS is clearly a much more powerful facility than SINQ, it is impressive how large the installation will be by comparison.

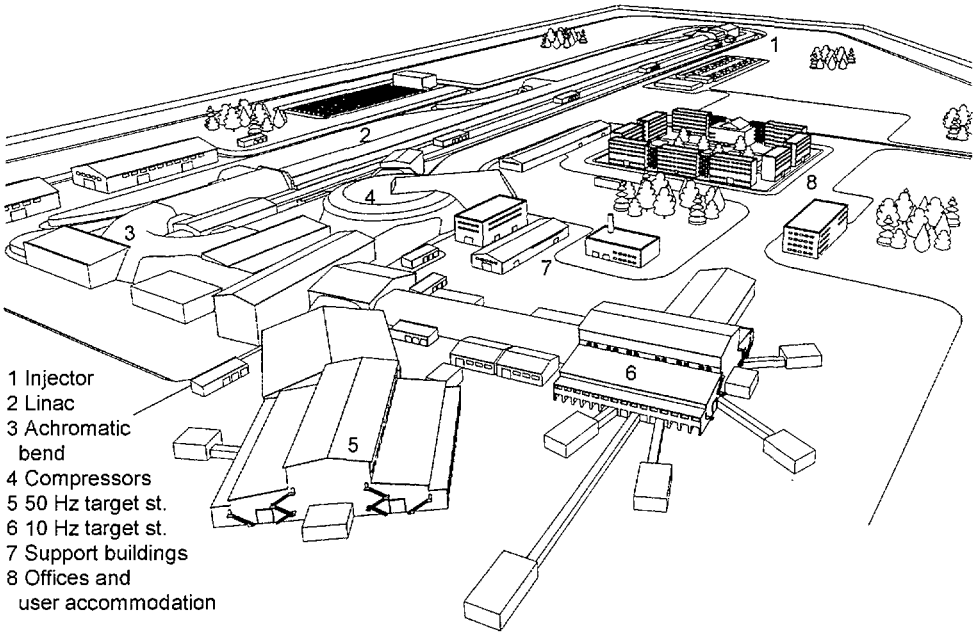

Figure 5-8 *Artists view of the ESS facility showing the linac building with an achromatic 180° bend leading to the compressor ring from where the beam is distributed to two target stations.*

The beam is injected into the ESS target horizontally, which not only makes the beam transport simpler and safer, but also has the advantage of an easier target handling system. Before entering the 50 Hz target station the beam passes through a large hall where the option has been left open to install other scientific instrumentation that might use part of the beam, similar to the situation at the PSI (cf. Fig. 5-2). This might either be meson targets or other test installations to carry out spallation related research.

5.2.2 The ESS target stations

The two target stations, although receiving different time average beam power will have to cope with the same proton pulses of 100 kJ energy content, which is a more stringent condition than an average power dissipation of 1 or 4 Megawatts. They will, therefore, be of essentially identical design, as far as the targets and their handling systems are concerned. Differences may result in the moderator layout and in the beam lines, because the low repetition rate target station is mainly intended for very slow neutron work, which requires longer separation between pulses to avoid frame overlap in time of flight measurements and, in order to optimize resolution, will occasionally also use very long flight paths. Good cryogenic moderators are, therefore, at a premium, and an initiative has been started, to develop an advanced system based on solid pellets of high slowing down power which are transported through the moderator vessel continuously to limit radiation damage and to release stored energy at regular intervals [10].
After some initial scoping studies [31], during which various target options, including rotating ones were considered, the ESS target team decided in favor of a liquid metal target using Mercury. It had become clear that the high absorption cross section of mercury for thermal neutrons is not a disadvantage for pulsed sources and that otherwise mercury has very favorable properties for use as a spallation material [32]. Among them are its high density, relatively low specific activation and the fact that it is liquid at room temperature and therefore does not require auxiliary heating or pose the risk of damaging the container by volume changes in the solid state. The horizontal beam injection and the liquid state at room temperature also favor a design concept [32], where the target container is surrounded by a separately cooled shroud that is connected to a dump tank in case the actual target container springs a leak or breaks. A schematic representation of the ESS Mercury target system is shown in Fig. 5-9.

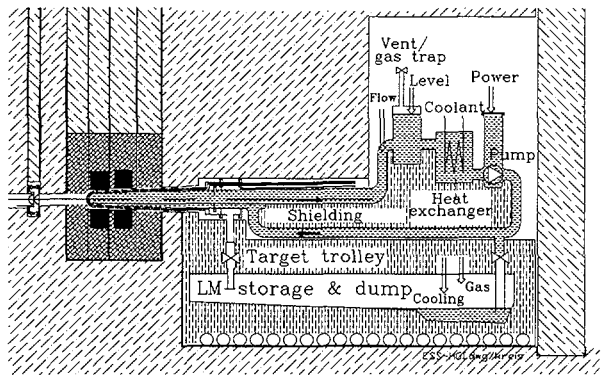

Figure 5-9 *Schematic representation of the ESS target system, mounted on a trolley that also contains the drain tank and can be rolled back into the hot cell for maintenance. The double walled protective shroud around the target is cooled separately and is connected to the drain tank to return spilled mercury in case of a leak in the container.*

The closed Mercury loop is mounted on a movable support to be able to roll it back from its operating position into a service hot cell for maintenance. The support trolley also contains a shielded drain tank into which the whole target loop can be emptied when breaking the container becomes necessary in order to exchange any component, in particular the snout that is exposed to the high radiation field during operation. This snout is surrounded by a separately cooled, double walled shroud which is connected to the drain tank and would allow to catch any mercury and return it to the drain tank safely, in case there would be a leak in the target container snout.
A cut away view of the target container and its surroundings is shown in Fig. 5-10. The small H_2O or supercritical H_2 moderators are located above and below the target and are viewed by horizontal beam tubes in a way that avoids direct sight on the target. The surrounding

reflector material is heavy water cooled Lead, in accordance with the discussion given in Chapter 3. A comparison with the SINQ target environment clearly reveals the difference in design principles between a continuous and a pulsed research spallation neutron source.

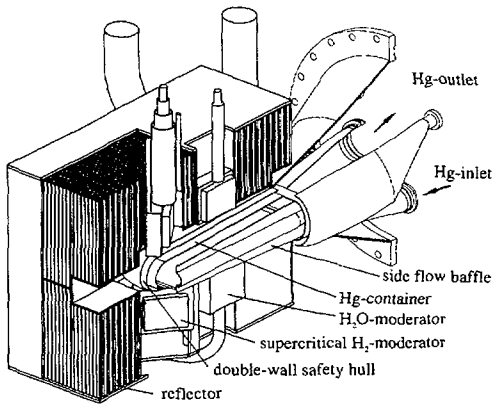

Figure 5-10: *The ESS Mercury target and its immediate environment of reflector and moderators.*

Computational fluid dynamics studies carried out to optimize the flow in the beam interaction area [33] showed that three inlet and one outlet channels for the mercury at the same time provide for sufficient window cooling and allow to reduce recirculation and vortex formation in the target region to a level which does not result in overheated zones. In this concept, the inlet flow through the bottom channel provides for the necessary flow across the beam window and the two side inlet channels provide the bulk of the mass flow and prevent recirculation in the beam interaction zone.

The plan view of the overall layout of the ESS target stations shown in Fig. 5.11 shows that the inner shielding block, which is essentially of steel and contains the beam shutter systems, is placed eccentrically in the overall shield to account for the anisotropy of fast neutron emission (Fig. 2-4) and the difficulty of shielding against these neutrons (cf. Ch. 6). In the forward direction relative to the proton beam the remote handling cell for the target loop will be located, in which also the moderator-reflector unit can be maintained. This unit, together with a large part of its shielding plug, must be lifted out of its operating position vertically and transported in a shielding cask to the maintenance cell through a high bay area on top of the target block.

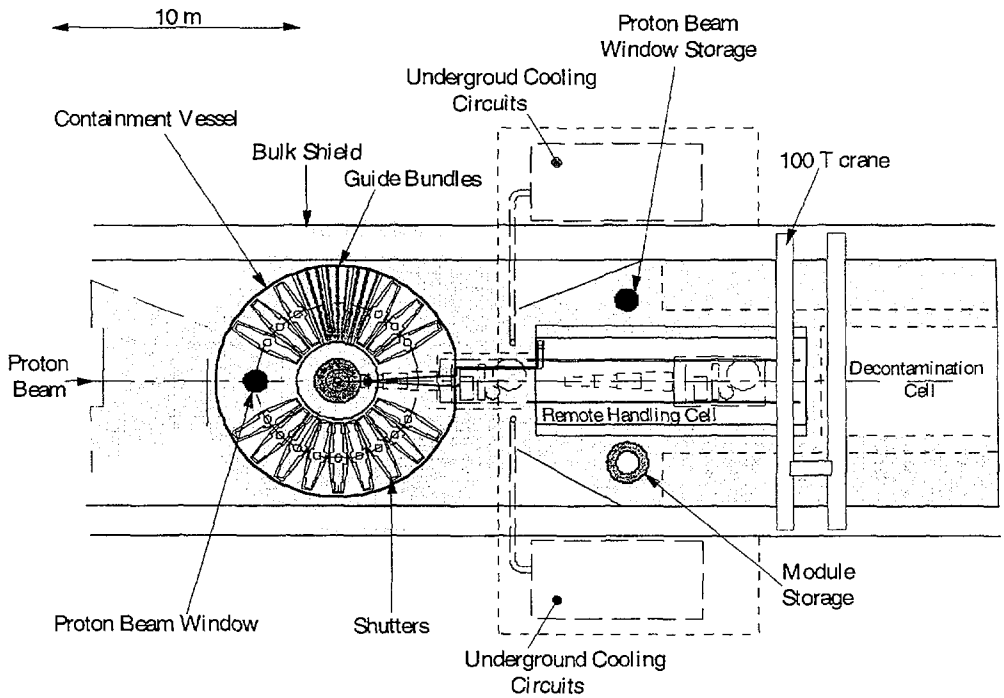

Figure 5-11 *Plan view of the overall layout of the ESS target stations*

Clearly, the need for a heavily shielded beam transport line and the service cells on the floor level and in immediate contact with the target block uses up a significant faction of the circumference of the target block, but the usually rather stretched geometry of instruments on pulsed sources and the extensive use of neutron guides will allow to accommodate nine direct beam lines on either side of the target, or even more, if neutron guide bundles can be employed. With its two target stations and high neutron flux (cf. Fig. 4-2 and Tab 5-1), ESS will be an extremely powerful facility, well suited to meet the users' demands to the next generation neutron sources. Its design and construction will, however, pose several technological challenges both on the accelerator as well as on the target side, and will generate a wealth of information relevant to possible future accelerator driven devices in nuclear technology.

6. Some Technology Issues and R&D Needs

6.1 Shielding

As can be seen from Fig. 5.3, the whole SINQ target and moderator region are embedded in massive steel and concrete and so is the ESS target-moderator reflector system. This is very different from the usual pool design of reactors, that makes access to the fuel and handling of fuel elements easy. The reason, why this is so can be seen from Figs 2.2 and 3.1, which show that the cross section of hydrogen and deuterium drop by two orders of magnitude in the region between 1 MeV and 100 MeV. Since this is a property of the nucleons it is true for all elements and, in order to obtain a reasonably short attenuation length, a high density of nucleons is required. So, not only pass high energy neutrons through water almost unmoderated, they are also very difficult to shield. This is particularly true in the forward half-space relative to the incident proton beam. This is the reason why the ESS target has been displaced from the center of the target block by 1.25m towards the proton beam (cf. Fig. 5-11).
Attenuation of high energy neutrons (above 15 MeV) in the shield is essentially by spallation, generating secondary particles also inside the shield. This is why, in the inner part of the shielding a buildup of dose occurs, before it decreases exponentially with an attenuation length λ. Clearly, calculating an optimized shielding is a very intricate task, because not only does deep penetration have to be taken into account, there are also combinations of many materials and complicated geometries that need to be considered, including streaming paths and imperfections in the construction of the shield. For scoping purposes in dose calculations, the relation

$$D(\theta) = \Omega \int dE \, \{\Phi(E,\theta)*F(E)*B(E) \, \Pi_i [\exp(-s_i/\lambda_i)], \quad (6.1)$$

where $D(\theta)$ is the dose at some angular position θ relative to the beam subtending a solid angle Ω to the source, $\Phi(E,\theta)$ is the source particle spectrum in that direction, F(E) is the flux-to-dose conversion factor and B(E) is the buildup factor mentioned above. The product of exponentials describes the dose absorption by the shield and takes into account stretches s_i of different materials with attenuation lengths λ_i.

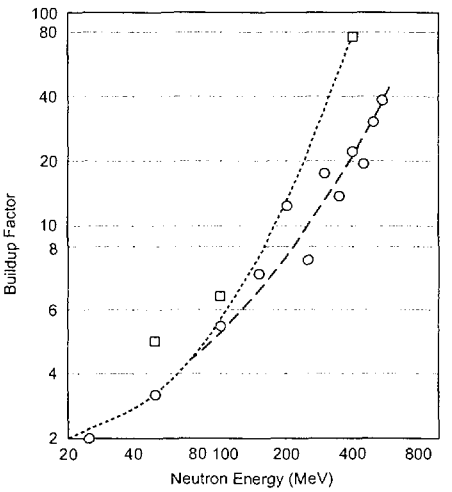

Figure 6-1 *The buildup factor for shielding calculations as a function of incident energy as obtained from Monte Carlo calculations [35] (circles), [36] (squares). Another factor of 2 should be added to account for the contribution of neutrons below 15 MeV [34]*

The purpose of the buildup factor B(E) is to be able to use the simple exponential attenuation formula for thick shields. It accounts, in a global way, for the production of secondary

particles inside the shield, for the fact that those particles traverse a shorter distance to the surface and for the fact that in high energy source calculations usually only neutrons above 15 MeV are accounted for. As can be seen from Fig. 6-1, B increases steeply with energy. It should be noted that an increase of B by a factor e requires 1 mean free pat more shielding at the outside, where this adds significantly to the volume and hence the cost of the shielding.

Also the shielding lengths λ_i are a function of energy and increase steeply up to a value of 100 MeV, as the nucleon cross section drops, as emphasized before. Above 300 MeV λ is roughly constant and is usually taken around 140 g/cm^2 for iron and concrete alike [34]. Of course, due to its higher density iron makes for a much thinner shield than concrete. However, pure iron has very pronounced minima in the cross section around 29 and 150 keV (the so called iron window), which means that neutrons, once scattered into this energy range, can travel very far and thus contribute significantly to the dose rate at the surface of an iron shield. This is why, apart from filling the gaps between the iron blocks in the SINQ shield with a special heavy mortar, a 30 cm thick layer of borated concrete was added to the outside. This takes care completely of the Iron window neutrons, since their energy is low enough to moderate and absorb them efficiently in the outer layer.
There is still considerable uncertainty about the best attenuation factors to be used for different shielding materials. In view of the fact that the main part of the cost foe a spallation target station is in the cost of the shielding, more and better defined measurements are urgently needed.
A comprehensive discussion of shielding calculations for spallation targets can be found in ref. [34].

6.2 Beam transport

Although accelerator technology is not a topic of this paper, the beam transport line and, in particular its last few meters in front of the target have a big influence on target and deserve some attention in the present context.

There is, of course, one direction in which shielding is particularly difficult, independent of the source concept: the proton beam channel. In order to keep the power density in the target at manageable levels, the beam footprint must be of a certain area, typically a few hundred cm^2. This is an open target surface through which a large number of fast neutrons are emitted, fortunately almost exclusively of energies below 20 MeV. Nevertheless, since no moderating or absorbing materials can be placed in the proton flight path, this neutron beam will lead to significant activation in the last several meters of the beam line. In the case of SINQ, three measures were taken to limit this activation:

(1) A neck is generated in the proton beam cross section some 3m below the target and a heavily cooled copper collimator is placed in that region which only leaves an opening of about 10 cm^2, thus limiting the cross section and solid angle of neutrons that can enter the proton beam line. (This collimator actually consists of three parts, as can be seen in Fig. 5.3, in order to optimize the position and minimize the amount of material used.)

(2) The last bending magnet in the beam line is of the C-type, allowing to place a branched vacuum tube in its gap which, on the one hand follows the proton beam path, but on the other has a vertical extension straight down to avoid scattering of the neutrons that have cleared the collimator in the wall of the vacuum tube.

(3) The vertical extension of the vacuum tube leads to a shielded beam catcher that can be replaced or removed if access is necessary to that area.

Since avoiding any ground water activation is a condition for obtaining an operating license, more shielding was buried in the ground under the beam catcher.
In order to accomplish a reasonably sharp bend of the rather fat beam, the last 60° bending magnet weighs about 60 tons without its support structure. This may serve to indicate what the choice of vertical injection implies. If vertical injection from above had been chosen, as discussed for some of the ADD-options, not only would this magnet have to sit stably above the target, it would also

have to be movable in order to get access to the beam injection tube for periodic replacement by remote handling.
One final remark to beam transport: Since designing the beam line for remote handling throughout is extremely difficult and expensive, one will always try to limit beam losses along the transport line as much as possible. This means that loss monitors will be placed in many locations, which trip the beam as soon as certain levels are exceeded. Unfortunately this is , in practice, one of the main reasons for beam interruptions at the PSI accelerator. It is, therefore important to design the beam line for a certain tolerance to slightly off-normal accelerator operating conditions, if frequent beam trips are to be avoided.

6.3 Radiation damage and operating temperature in target and structural materials

Radiation effects are very well studied in fission and fusion reactor materials, and a general image has evolved on what kind of changes are to be expected under certain irradiation conditions. They are all consequences of two kinds of interactions of the radiation field with the material:

(a) Nuclear interactions which can lead to significant alterations of the materials composition. While in fission and fusion reactor spectra, whose neutrons have energies below 14 MeV only, this is predominantly neutron capture and secondary reactions from the decay of radioactive products, the spallation spectrum containing high energy protons and neutrons up to several a GeV will generate a much broader range of reaction products (cf. the example given for PbBi in Fig. 2-5). In particular, the cross section for Hydrogen and Helium production increases steeply with neutron energy (and atomic mass), resulting in much higher production rates of these species in a spallation spectrum. Being light gases, they can diffuse through the lattice relatively easy, which may lead to segregation to grain boundaries or gas bubble formation and have a strong effect on the mechanical properties of the material. Of course also enhanced the mobility of other species may be important, especially in alloys that have been stabilized in a certain state, i.e. contain metastable structures. This enhancement comes from the second kind of interaction of the radiation field with matter: atomic displacements.

(b) Atomic interaction by transfer of kinetic energy to individual atoms of the solid („primary knock-ons") which, as a consequence, can be displaced from their lattice site and can, if their energy is high enough, displace also other atoms from their positions, thus creating a cascade of damage in a small area in the solid. In this cascade region, there will be empty lattice sites („vacancies") and atoms that come to rest at positions, which are not regular lattice sites („interstitials"). Many of the initially created vacancy-interstitial pairs will recombine while the lattice is still locally very „hot", i.e. the atoms are vividly oscillating. Thus, the net number of lattice defects remaining is much smaller, than the number of atoms actually displaced from their sites. This is why, after tens of „displacements per atom" (dpa), the lattice can still be more or less in tact. Therefore, the dpa-level, which is commonly used as a measure of radiation damage is not a scientifically justified scale. It is calculated on the basis of the total energy transferred to the material divided by the mean energy required to displace one atom from its site in the particular material. Nevertheless, the dpa number has proved as a useful reference to characterize the amount of radiation a material had been exposed to, accounting for its microscopic properties to some extent.

The temperature of irradiation is, of course, an important factor. One reason is the amount of spontaneous recombination. Another one is the mobility of certain species in the lattice mentioned above, which is strongly temperature dependent. It has been found that, based on their reduced irradiation temperature, most metals show the same kinds of reactions to irradiation. This is shown in Fig. 6-2 (after [37]). This shows that above 80% of the absolute melting temperature, practically no radiation effects ar to be anticipated. Running a target in this temperature range means that mechanical strength must not be an issue, because it

decreases rapidly for most materials at those temperatures. It is, however conceivable in principle, to run solid targets in that temperature range, if a suitable design is chosen. For example, Lead) when irradiated at 200°C will, if any, suffer from Helium embrittlement only (Fig. 6-2. In the SINQ development plan it is foreseen to use Lead in tubes of martensitic steel, which provide the required mechanical strength. According to calculations and first tests the temperature will run well above 150°C at 1 mA, which is the upper limit of void swelling. It should be noted, however, that there will always be a large range of temperatures in a target and irradiation conditions will, therefore, vary locally. This is particularly important if one tries to run, for example a beam window, above the hardening regime in the beam center: Towards the edges of the beam the temperature will always be lower and creep in the ductile center may result in reversed stress when the beam is turned off. So, clearly one must be very careful when judging the situation only by the most highly loaded point; the regions around it may be in more of a risk than the hot spot itself.

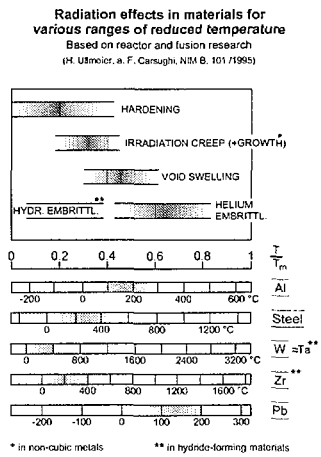

Figure 6-2 *Radiation effects in materials as a function of reduced temperature, based on results from fission and fusion spectrum irradiations. The usual ranges of operating temperatures are indicated for some target and structural materials. (after [37]).*

Of course, the degree to which the effects listed in Fig. 6-2 play a role depends very strongly on the particular material in question. Several steels have been developed, that are fairly resistant to radiation damage and also some Aluminum alloys have been used to several tens of dpa. Unfortunately Tungsten and its machinable alloys, like W5%Re, otherwise favored target materials, seem to suffer from a rapid increase of its ductile-to-brittle transition temperature under irradiation [38]. As mentioned before, until recently there were almost no data on the effects of spallation radiation on materials, but with the recent interest in powerful spallation sources and with the advent of suitable opportunities, such as the LASREF-facility at Los Alamos, used now mainly in conjunction with the APT-project [39],[40] and the SINQ target irradiation program [41], this situation is now rapidly changing. Also, first components used over long time in existing facilities have now become available for examination [42]. These were mostly intensely water cooled components, so their irradiation temperature was generally low. Nevertheless, first results give quite interesting data on the behavior of different kinds of steel and will be published soon [43]. They show that, while for martensitic steel of the DIN 1.4926-type the hardness increases, but it retains significant ductility up to 6 dpa, the hardness of the artificially hardened Iconel 718 decreases and it is severely embrittled in the same load regime. This clearly demonstrates that it is important to have data for exactly the materials and operating conditions in question. One important feature in spallation neutron sources are the frequent large amplitude thermal cycles due to accelerator trips that seem to be difficult to avoid.

6.4 Heat removal and radioactivity in solid targets

Apart from Lead, which has a fairly „low" density and therefore is considered mainly for continuous spallation sources, the two solid target materials for pulsed sources are Tantalum and Tungsten, both of which excel by high melting points and high density. Of these, Tungsten is probably the most desirable one because it gives the highest neutron leakage per unit area and unit beam power due to its low resonant absorption. Relative to Tantalum there is about a 20% gain (Fig. 6-3). At the same time, its afterheat

and radioactivity is significantly lower than for Tungsten (Fig. 6-4).

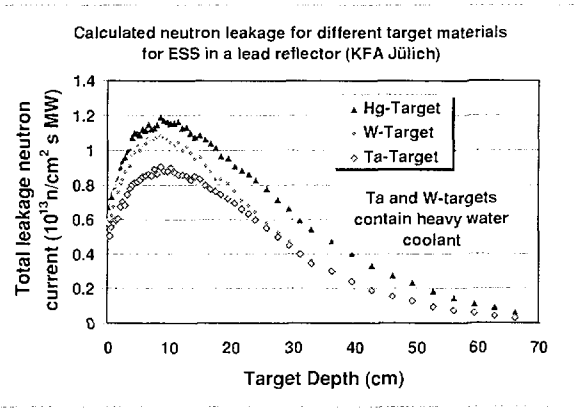

Figure 6-3 *Calculated neutron yield for Tungsten, Tantalum (both with 20% coolant fraction) and Mercury targets in a large lead reflector [47].*

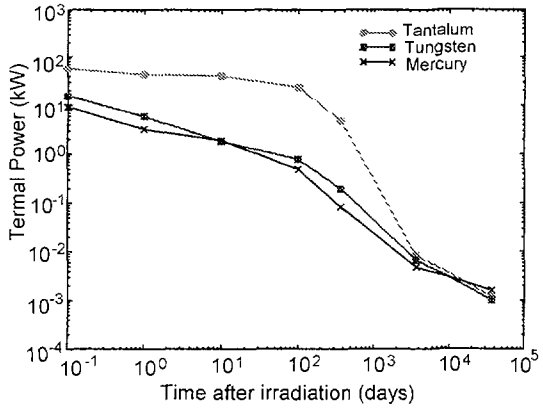

Figure 6-4 *Calculated afterheat for Tungsten, Tantalum and Mercury targets after 200 days of operation in a 5 MW beam [47])*

One problem, apart from its brittleness, is the fact that, under irradiation, Tungsten is rather seriously corroded by water [44] and that it can be shaped by powder metallurgy only. Machinable W-alloys have also be found to be susceptible to water corrosion. No experience seems to exist in this respect with W-Re alloys, which are ductile at room temperature but seem to embrittle rather rapidly under irradiation [38]. The currently most powerful pulsed spallation source, ISIS has, therefore, been using a Tantalum target, but efforts have been successful, to develop Ta-clad W-plates, which will be tested in future targets [45].

The ISIS target is a surface cooled plate target with flat plates of increasing thickness, as the power density deposited by the beam decreases along the target axis (Fig. 6-5)
Heat removal from solid targets is limited by two factors:

- heat conduction in the solid; The need to limit the center line temperature and the surface temperature of the plates or rods in a solid target determines the maximum thickness of the target material. In a 1-D approximation (heat flux perpendicular to the target surface only) the amount of heat that must be removed per unit surface area in a plate target is given by the power density Q times half the thickness d of the plate (2-sided cooling). Assuming that the mean distance of heat transport is half of the heated region (d/4) the heat flux on the surface is

$$q = Q \cdot d/2 = h \cdot (T_w - T_L). \qquad (6.2)$$

T_w and T_L being the wall and coolant temperatures and h the heat transfer coefficient, which depends on the type of surface and the flow via Nusselt's number Nu, To determine Nu, a frequently used correlation is the one by Dittus-Boelter, that relates the heat transfer coefficient to the Reynolds- and Prandtl numbers of the flow channel.
The temperature drop from the plate center to the surface becomes

$$T_{max} - T_w = \frac{1}{8\lambda_s} \cdot Q \cdot d^2 \qquad (6.3)$$

and for the surface wall stress one obtains:

$$\tau_s = \frac{\alpha \cdot E}{12\lambda_s(1-\nu)} \cdot Q \cdot d^2 = \frac{2\alpha E}{3(1-\nu)}(T_{max} - T_w) \qquad (6.4)$$

Here E is the elastic modulus. λ_s the thermal conductivity, α the coefficient of linear expansion and ν Poisson's ratio.

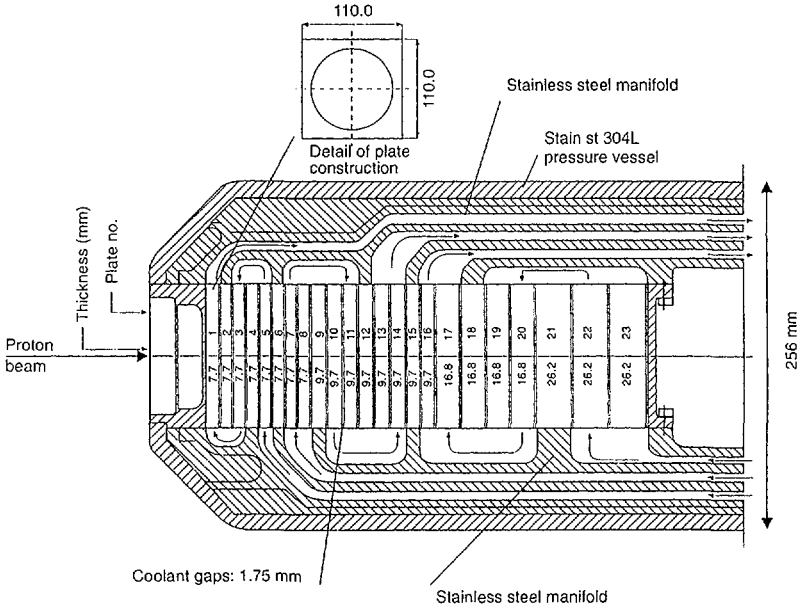

Figure 6-5 *The ISIS solid plate target*

In simple terms: one has two boundary conditions, (6.2) and (6.4), for the heat flux through a surface of the solid target and, depending on the operating regime, one of the two will be effective. This can be easily seen by plotting both in a log-log plot of Q versus d, which results in two straight lines of slopes -1 and -2 (Fig. 6-6).
Traditionally, in order to avoid parallel channel flow instability, one always tries to suppress boiling at any point of the plates, although, with the onset of nucleate boiling heat removal becomes much more efficient, and at least an order of magnitude more heat can be removed before the critical heat flux is approached, where burn out occurs (Fig. 6-7).

In Fig. 6-8 [46] the result of an analysis based on the above considerations is shown for a W-plate target to be used at an 0.6 MW, 3 GeV beam whose peak heat flux density along the axis is represented by (cf. eq. (2.5)) $\hat{Q}(z) = 1603\left[1-\exp\left\{-(z+1.9)/4.7\right\}\right]\exp(-z/116)$, with z in mm and Q in MW/(m^3 MW$_{beam}$).
The transition from the convection-controlled to the conduction-controlled cooling region occurs at the point, where the peak temperature in the solid reaches 538 °C, which was set as the upper permissible limit.

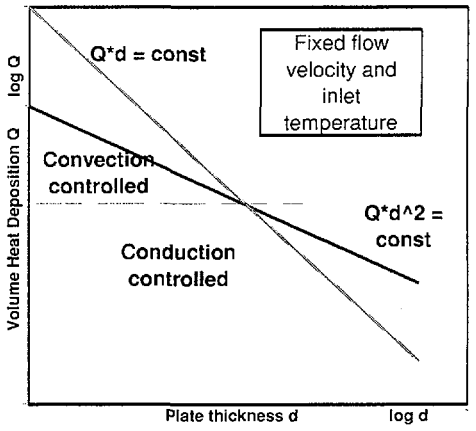

Figure 6-6 *The heat transfer limitations in plate target design.*

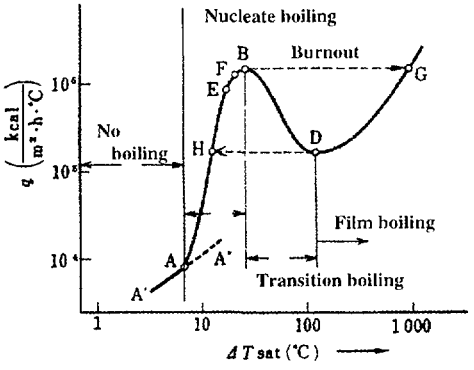

Figure 6-7: *The boiling curve: A: onset of nucleate boiling; E: departure from nucleate boiling; B: burnout point; Conventional design stays below point A.*

It can be seen that at the front of the target the resulting plate thickness becomes very small, of the order of 5 mm, due to the convective heat flux limitation of 300 MW/m^2 imposed. With a coolant gap of 1.5 mm this results in a significant water fraction in the volume.

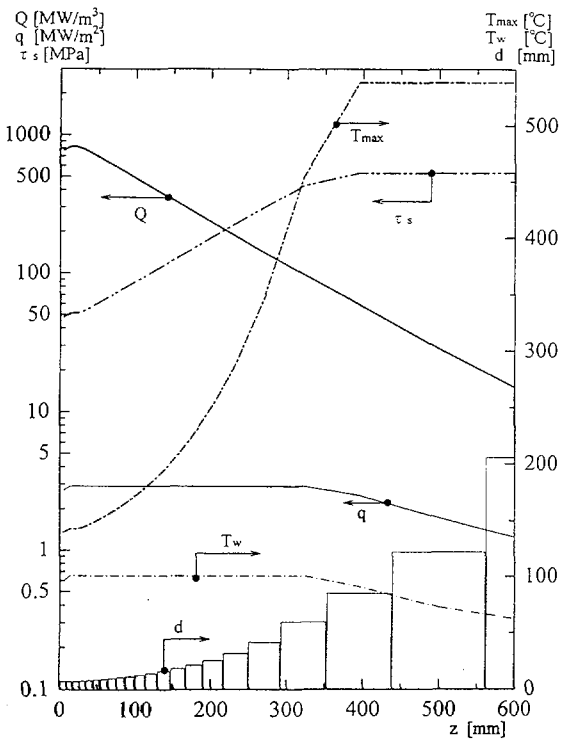

Figure 6-8: *1D-design of a 600 kW plate target [46]. Flow velocity in the cooling channels 10 m/s; wall temperature 100°C, max. allowed center temperature 538°C; allowed heat flux density 300 MW/m^2.;Up to the transition from convection limited to conduction limited the heat flux is constant, above the transition T_{max} is constant*

The water fraction in the target volume is important not only because of its diluting effect on the overall target material density, but also because of the radioactivity level in the cooling channels. Mainly the production of ^{7}Be by spallation of oxygen is a nuisance in the cooling loops on an intermediate time scale, because of its half life of 53 days and because it plates out completely on the walls of the pipework [47], making access to the cooling plant room difficult within a short time after shut down. Other radioactive isotopes of short half life generated in the cooling water or injected from the cooled walls produce a very high radiation level (up to 1 Sv/h at certain positions at SINQ [47]), which are a problem with respect to the materials that can be used in the loops (valves, sensors etc.) concerning their radiation resistance.

In this context it may be worth mentioning that in the AUSTRON project [48] an edge cooled solid Tungsten target is foreseen that would have no cooling water in the direct beam but would run at center temperatures above 1000°C already at a beam power of 250 kW, as originally proposed. According to Fig. 6-2 this would be just above the hardening limit at the lower region of void swelling for Tungsten. But, as discussed in the previous chapter, the whole temperature range down to the 300°C prevailing at the edges would be present. With recent plans to increase the beam power to 410 kW, it seems worth-while to consider changing the concept from an intensely coupled cooling system to a loosely coupled one [49]. While this would result in even higher temperatures, there would be less gradient in the target and, by employing a temperature dependent heat transfer barrier, thermal quenches could be kept much less serious. In an extreme case this barrier could be thermal radiation, which goes as the difference of the fourth powers of the temperatures of the sending and receiving surface. There are, however, other solutions, such as boiling metal heat transfer plates, which are now used to eliminate temperature gradients inside furnaces [50] and can be made to operate at temperatures up to nearly 2000K with proper materials combinations. Of course, other consequences of the high operating temperature, such as gas release must also be studied.

A factor, which has not played an important role in existing spallation targets, because of their relatively low power is afterheat removal in a loss of coolant incident. As shown in Fig. 6-4, the decay heat of a Tantalum target is of the order of 16 kW/MW$_{beam}$ at shutdown and stays high for about 100 days. Since the volume of a solid target is rather small, of the order of a few liters, and since the distribution of afterheat inside this volume is very inhomogeneous, with little heat exchange between plates, the local temperature may quickly rise above the point where backfilling with cooling water becomes impossible due to steam blockage. Although the situation is less severe with Tungsten this is another reason

why, at high power levels, solid targets become increasingly difficult and will probably require a second independent heat removal system as the beam power goes up. (It may be worth noting, that the ISIS target has such a system in that the top and bottom plates of the target casing are cooled independently of the target. The SINQ target also has an independent cooling loop for its container shell and provisions have been made to keep the target flooded at all times even after the event of a simultaneous failure of both walls of the containment shell.)

6.5 Liquid metal targets

Presently there is general consensus among target developers that up to 1MW of beam power solid targets are feasible from a heat removal point of view, but their limits will be not too far above this level. For higher power levels liquid metal targets are the option of choice. Apart from their higher heat removal capability due to the fact that the heated material is transported rather than the heat, they offer a number of potential advantages over volume cooled solid targets, most if which have already become obvious in the preceding chapters:

1. Higher spallation material density in the volume due to absence of cooling channels which tend to dilute the target the more, the higher the power density.
2. No or a minimum amount of water with its associated problems in the proton beam.
3. No life time limit caused by radiation damage in the target material. Only the structural material, which need not be chosen for high neutron production but can be selected for high radiation resistance, will suffer from this effect.
4. Significantly lower specific radioactivity in the target material due to the large mass used and perfect mixing, making an emergency cooling system unnecessary and allowing afterheat removal by very simple means in a region where it does not affect the design of the neutron source proper.
5. The inside pressure in the target can be significantly lower than in a water cooled system, putting less stringet requirements on the casing wall thickness.

Of course, the significance of all these arguments increases with increasing beam power.

Since liquid metal targets are a novel concept, there is no pertinent experience and a number of issues must be considered. The choice of materials is very limited and has already been given in Tab. 5-2: Lead based liquid metal targets will be good, if high operating temperatures can be afforded (or are desirable) an if thermal neutron absorption in the target should be low. For low operating temperatures and when a high fast flux is the main goal, Mercury can be used. In many respects all heavy liquid metals are similar, but there are differences, for example in their wetting behavior towards solids, the solubility of foreign species etc., which may affect practical details of their use. This concerns heat transfer from and to walls, which is important for the cooling efficiency for beam windows and the sizing of heat removal systems. In the following, we will touch upon some of the issues that need to be looked at without, however, being able to give clear answers in most of the cases.

6.5.1 Liquid Metal-Solid Metal Reactions

Although, from the point of view of radiation damage in structural materials there may be arguments to select somewhat elevated operating temperatures, one will generally try to run spallation source targets, at least for research neutron sources, at as low a temperature as compatible with the need of avoiding freezing for a variety of reasons. Nevertheless, there will be a hot spot at the beam entrance window and a cool region at the heat exchanger. This might, in principle, give rise to one or both of two phenomena: Liquid metal corrosion and liquid metal embrittlement. The state of knowledge, poor as it is, has recently been reviewed [51] and only a brief account will be given here.

Liquid metal corrosion is effectively a mass transport phenomenon from hot to cold regions of the loop. It can happen if the wall material or one of its major constituents has a highly temperature dependent solubility in the liquid. In that case dissolution will occur at the hot point and at the cooler parts of the loop the dissolved component will segregate to the

walls. This leads to weakening of the material in the hot regions on the one hand and may result in flow bolckage in the heat exchanger on the other. Although no data seem to be available for the temperatures in question, some information may be drawn from data on higher temperatures. Of the major constituents of steel, Iron has a low and weakly temperature dependent solubility in Mercury and also in Bismuth its solubility is lower than that of Chromium and Nickel The solubility of Nickel, is highest in both liquid metals, although in Mercury it has only a weak temperature dependence. The temperature dependence of the solubility of Chromium in Mercury is stronger than that of the other two. As a consequence it is even lower than that of Iron below 450°C. Based on these findings, low Nickel content steels were selected as preferred candidates for the containers of the SINQ and ESS targets, although the argument does not seem to be very strong. A summary plot shown in Fig. 6.9 [52], seems to indicate that, at total concentrations of Ni, Cr and Mn of less than 15 %, no severe corrosive attack must be anticipated for steels at temperatures up to 500°C by Mercury.

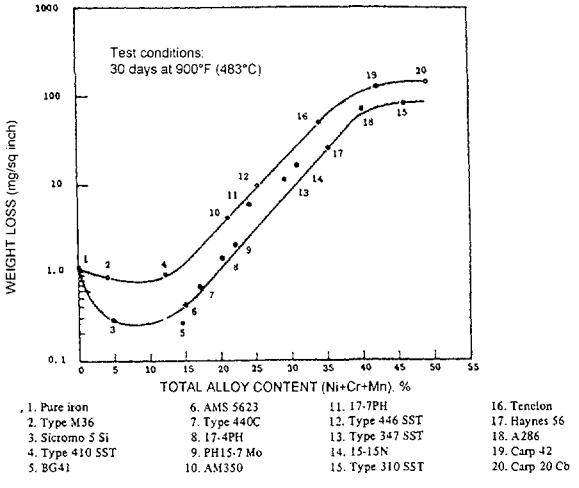

Figure 6-9: *Summary plot of the corrosion of steels in Mercury as a function of their total content in Ni, Cr and Mn.*

Particularly low corrosion rates were observed for 5%Cr-0.5%Mo-1%Si low carbon steel [53]. Furthermore, it was reported that steel with high nitrogen or carbon content were efficiently protected from corrosion if Zr or Ti was present in solution in the Mercury, probably due to the formation of insoluble Ti- and Zr-carbides or nitrides on the surface. In summary, at least without possible amplification effects of simultaneous stress and irradiation, corrosion by Mercury is not expected to be a problem for a properly chosen container material, for which a rather wide selection seems to exist.

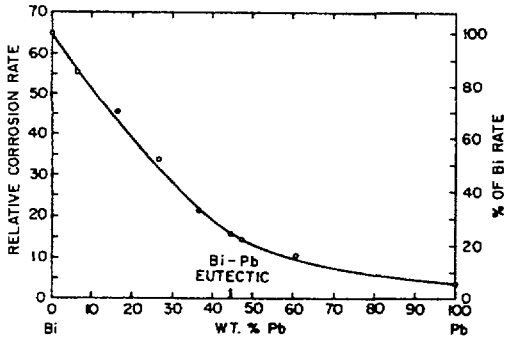

Figure 6-10: *Estimated dependence of the effect of Bi-concentration in Pb-Bi on the corrosion rate of steels for a temperature interval of 650-500°C.*

By contrast, bismuth seems to be a much more aggressive material than both, Mercury and Lead. In Lead-Bismuth mixtures the corrosion rate depends strongly on the Bi-content. An estimated dependence of the relative corrosion rate for the temperature interval between 650 to 500°C is shown in Fig. 6.10. An extremely strong temperature dependence seems to exist for the corrosion by PbBi-eutectic: While at a 625-500°C temperature interval a ½-inch pipe was blocked in 80 hours with no special measures taken, no blockage was observed at 400-200°C after 10 000 hours, when the experiment was terminated [54]. An important factor in the corrosion by Lead-Bismuth seems to be the oxygen content. Oxygen can form oxide layers on the surface of steels, especially at high Chromium content, which reduce corrosion rates, if they can be maintained stable. On the other hand, Pb- and Bi-oxides are slightly soluble in PbBi-etectic, which can lead to reduction of the Fe- and Cr-oxides at the hot spot and to deposition of Pb- and Bi-oxides in the heat exchanger. Precise control of the oxygen content has, therefore, been identified as a key issue in safe operation of the PbBi-cooled Russian nuclear submarines [55]. With this measure, corrosion has been successfully prevented in these systems. So, in summary, in particular at

moderate temperature levels, even corrosion by PbBi-eutectic does not seem to pose serious problems for steels with low Nickel and high Chromium content.

Liquid metal embrittlement is a well known phenomenon, for example for Aluminum and Mercury. It has been observed preferentially in systems, where the solid and the liquid metal do not form intermetallic compounds [56] but other cases have been reported, too [57]. From simple thermodynamic arguments it was concluded [56] that binary systems in which liquid metal embrittlement is most likely to occur have a low temperature dependence of the solubility of the solid component in the liquid, which is precisely what one would choose to minimize corrosion. In contrast to corrosion, liquid metal embrittlement does not depend on a temperature gradient in the liquid, but may be strongly affected by the temperature level.

The reason why liquid metal embrittlement is a particular concern is because it is strongly affected by stress on the solid. Phenomenologically it is explained by a liquid-solid bond which is strong enough to weaken the solid-solid bond to a level below or near the yield strength of the solid metal. Any stress on the solid may thus lead to crack propagation, often along grain boundaries where the order is perturbed or where foreign atoms may catalyze the process. The phenomenon does not imply transport of dissolved atoms over long distances, but rather a rearrangement in the immediate vicinity of the tip of the propagating crack. It has certain similarities with the well known phenomenon of stress corrosion cracking, which is also known to be "assisted" by irradiation (irradiation assisted stress corrosion cracking, IASCC). However, no information at all seems to exist on the influence of simultaneous irradiation and stress for liquid metal embrittlement.

In contrast to radiation embrittlement, liquid metal embrittlement does not go along with hardening, nor does it affect the whole volume simultaneously. It is effectively a weakening of the grain boundaries that progresses from the surface and reduces the stress bearing thickness of the material. So, while radiation embrittlement can lead to enhanced crack propagation, if such cracks are present, but otherwise does not have a negative effect on the elastic properties of most materials, liquid metal embrittlement will eventually lead to component failure, even if the design originally was very conservative with respect to the elastic stress regime.

The above remarks need not mean that there is a high risk for liquid metal embrittlement or corrosion to destroy the target container, even under its rather severe operating conditions, especially since low nickel content martensitic steels are favored for the SINQ and ESS target containers. There simply isn't enough information available to judge the situation reliably, and serious R&D work is needed on this topic.

6.5.2 Pulsed power input

Since short pulses are a prime design goal in pulsed sources, the effect is that the time average power of perfectly manageable level is deposited in large "chunks". Even for a high repetition rate source as ESS, the power in one proton pulse is 100 kJ and about 60% of this is deposited in a small volume of the order of a few liters during 1 μs. It was pointed out immediately when Mercury was first proposed as target material for ESS, that this was the source of potential problem [58]: During the short heating time the liquid has no way of accommodating the resulting expansion by displacement conduction or convection and hence a high pressure level builds up which is the source of a pressure wave traveling outward and eventually hitting the container, where it generates dilatational stress. In the following, the whole system will experience pressure and stress oscillations until the energy has been dissipated. Although the exact magnitude of this effect depends on geometric and other design details and on position, its order of magnitude could be readily calculated for a cylindrical geometry and it was found to be in a regime, where the endurance limit of the container material might play a role. A more detailed analysis was carried out later [59], taking into account the direct power deposition in the beam window as well as that in the liquid metal. The calculations showed that, from the direct heat input in the window rather high stress levels perpendicular to the wall surface resulted and that a high frequency stress wave starts to travel along the wall as soon as the pulse

occurs. By comparison, the pressure wave from the liquid arrives at the surface only at a later time, depending on the distance it has to travel, an it generates a lower frequency of oscillation. These calculations also allowed to take into account the effect of possible voiding (cavitation) in the liquid metal, i.e. the failure to sustain tensile stress. If voiding was to occur at zero pressure, i.e. the fluid had no tensile strength at all, this would, under certain conditions, result in a roughly two times higher stress than if no voiding would occur at all.
One way considered to mitigate the effect of these pressure waves was to try and inject gas bubbles in a suitable distribution in order to "soften" the liquid metal, i.e. increase its compressibility. It was found that, if the compressibility was the average of the static compressibilities of the two compounds, the magnitude of the wall stress would be reduced to 10% or less of the value for the "pure" liquid metal at a gas concentration around 3 vol%. Although efforts are going on at the ESS project to generate such bubbles in the liquid metal, one must be careful about using static properties for the highly dynamics effects in question. At the time being, gas injection can not yet be considered as a safe way to control the pressure wave problem. In an attempt to obtain experimental information, an international collaboration was organized to carry out full power measurements on a full scale target on the alternating gradient synchrotron in Brookhaven, which is just producing first results that allow to validate calculations in the gas-free case and seem to indicate that, at least at 30 kW pulse power voiding does not happen.

6.5.3 Liquid Metal Pumping and Heat Removal

Both, pumping the liquid metal and removing the heat are not considered a principal problem, they are more a matter of practicality and of optimum design, depending on the temperature range in question and other boundary conditions. Both, mechanical and electromagnetic pumps have been used successfully for heavy liquid metals. While mechanical pumps must be of special design to ensure completely hermetical enclosure of the liquid metal, this is naturally the case for electromagnetic pumps. The latter are much more voluminous and have rather poor efficiency, of the order of 10% for PbBi or Hg, which results in significant heating of the material. This heat input need not be a disadvantage because, by comparison to the beam power, it is still low but may be helpful in keeping the liquid metal warm when the beam goes off. This is, of course, of particular importance for Pb-based targets which could freeze in the event of continued heat removal with no beam. For the SINQ target two passive measures are being studied to keep the target from freezing during short and medium long beam trips without having to activate the auxiliary heating, which is an active device, each time:

(1) A pumped flow of liquid metal which is only a fraction of the total flow required to remove the heat will be directed across the beam window to ensure its proper cooling at all times and to maintain a minimum circulation in the loop without beam. An important part of the liquid metal movement will, however, come from natural convection, which is input power dependent and thus matches the heat removal rate to the heat input rate at the reaction zone.

(2) A system of variable conductance heat pipes is studied [60], which operates at a temperature range around 200 °C and stops heat transport when the temperature level drops below 165 °C by the expansion of a non-condensable gas volume as the temperature and hence the pressure of the heat transport fluid (H_2O) decreases.

In this way not only should freezing of the Lead-Bismuth eutectic be safely avoided during short beam trips, it should also be possible to use the present low pressure water loops to ultimately remove the heat from the target by back-cooling the heat pipes.

6.5.4 Production and Release of Polonium in Lead and Bismuth

Apart from its different operating temperature and neutron absorption, Mercury has the important advantage that virtually no α-active ^{210}Po is produced in it. This is not true for Pb and, in particular for Bi where ^{210}Po can even

be produced by double neutron capture. It has been estimated for the particular operating conditions of SINQ [61] that in a Pb-Bi target there would be roughly 1000 times more ^{210}Po produced than in a Pb-target. This has, for some time, resulted in reflections to use Lead instead of Lead-Bismuth for SINQ. However, as can be seen from Table 5-2, this requires significantly higher operating temperatures, even if the Pb-Mg eutectic were used, which has a very narrow compositional range of reduced melting temperature. From the work carried out for the ISTC-project No. 17 [62], it is known that Po escapes from Pb-alloys as PbPo and the evaporation rate can be described by

$$q = m^*q0 = m^*K^*p(T)^*\sqrt{(M/T)} \qquad (6.5)$$

with $M_{PbPo} = 418$, $\log(p(T)) = 6.64 - 7270/T$ and $K = 0.438$ kg/m^2/s/mbar

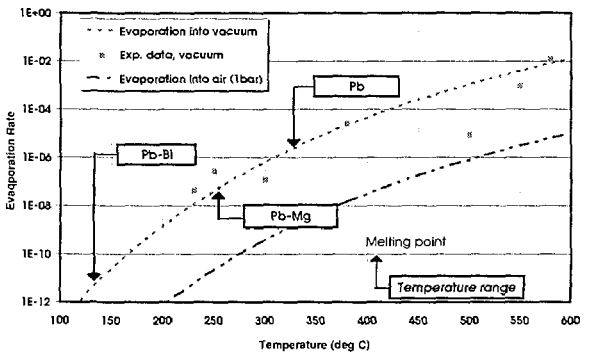

Figure 6-11:*Evaporation rates of polonides into vacuum and air as a function of temperature. Vertical arrows indicate melting points of different Lead alloys and the boxes represent the operating temperature range.*

The corresponding curve is plotted in Fig. 6-11, for both, evaporation into vacuum and into air at 1 atm. The operating temperatures of LME, LBE and Pb are indicated by boxes and the melting points by vertical arrows It follows that, from PbBi and PbMg targets about the same amount of Po would evaporate, whereas this number is about a factor of 60 higher for pure Pb, even accounting for a 1000 lower concentration in PbMg and Pb than in PbBi. Clearly, being a short range α-emitter, ^{210}Po is not a problem as long as it is confined in the liquid or solid metal. So, from this point of view there is no incentive to use lead if the operating temperature can be chosen low. It should also be noted that the high ^{210}Po in PbBi results from the high thermal neutron flux which surrounds the target in SINQ. The situation can be very different in different configurations.

7. Concluding Remarks

There is no question that research neutron sources deserve the credit of having pioneered the use of accelerators in nuclear technology and, in 25 years of its existence, the International Collaboration on Advanced Neutron Sources ICANS [63], has generated a wealth of information on spallation target technology and accelerators apart from developing novel techniques for the use of pulsed neutron sources. The presentations given at fourteen meetings of this collaboration have been documented in the respective proceedings, published regularly by the hosting laboratories. These volumes now represent a valuable source of information. Although some cross connections existed on and off, research spallation sources have, in general, not been considered as technology test beds for large accelerator driven devices. To some extent this seems to be changing now, as laboratories, like JAERI are proposing to build neutron science centers [64] as a development stage and test bed for higher power ADT.

In view of the large amount of development work required, this research is on the verge entering the status of true and organized international collaborations. The Neutron Sources Group of the OECD Megascience Forum has drafted corresponding recommendations, which, hopefully, will give further momentum to this move. Meanwhile, some dedicated R&D-collaborations are forming, such as ASTE (AGS Spallation Target Experiment) [65], ACoM (Advanced Cold Moderators) [66] and SIP (SINQ Irradiation Program) [67], where laboratories from many countries actively join efforts to reach a common goal.

An important issue on which little progress has been made so far is the effect of simultaneous irradiation and stress on solid-liquid metal interactions. The probably most comprehensive work would be possible by utilizing the irradiation facility in the Moscow Meson Factory, for which a plan has been

worked out [68]. As a preliminary test the possibility is being explored to use the 72 MeV Phillips cyclotron at PSI to irradiate a solid-liquid interface under thermal stress [69]. It has been shown that, while neutron production and the resulting activation is low at that proton energy, H/dpa and He/dpa ratios are reasonably high and realistic power densities can be achieved. Also the dpa rate per proton is not far from its value at higher proton energies and the time to reach about 10^{21} p/cm^2, corresponding to 2 dpa, is roughly 20 days. These conditions are considered adequate to carry out preliminary tests in order to see whether any effect is found.

Based on the results from such work one can anticipate that research spallation sources, in the near future, will not only cross the 1 MW beam power level, but will take the technology across the 5 MW barrier. As shown in this paper, this will require new technologies of immediate relevance for ADD-development.

8. References

[1] G.J. Russell, "Spallation Physics-An Overview"; Proc. ICANS-XI, Tsukuba, 1990 KEK-report 90-25 (1991) p.291-299

[2] S. Cierjacks, F. Raupp, S.D. Howe, Y. Hino, M.T. Swinhoe, M.T. Rainbow, L. Buth "High Energy Particle Spectra from Spallation Targets" Proceedings ICANS-V, KFA Jülich, 1981; Report Jül-Conf-45 (1981)p. 215-240

[3] V.I. Yurevitch, "Review and Analysis of the Experimental Data on Neutron Production in Lead Targets Obtained at p/d-Beam of the Dubna Synchrophasotron During 1986-1992"; Preprint, private comm.

[4] R.G. Vassil'kov, V.Y. Yurevich, V.G. Khoplin „Neutron Emission from an Extended Lead Target under the Action of Light Ions in the GeV Region" Proc. ICANS-XI, Tsukuba, 1990 KEK-report 90-25 (1991), pp 340-353

[5] L. Pienkowski, F. Goldenbau,, D. Hilscher, U. Jahnke, J. Galin and B. Lott, "Neutron multiplicity distributions for 1.94 to 5 GeV/c proton-, antiproton-, pion, kaon-, and deuteron-induced spallation reactions on thin and thick targets" Phys. Rev. C 56 1909 (1997)

[6] F. Atchison Nuclide Production in the SINQ Target SIN report SINQ/816/AFN-702 (1997)

[7] J.M. Carpenter and W.B. Yelon, "Neutron Sources"; in "Methods of Experimental Physics" 28A p. 99-196 Academic Press (1986)

[8] G.S. Bauer "Pulsed Neutron Source Cold Moderators - Concepts, Design and Engineering" Proc Int. Workshop on Cold Modeators for Pulsed Neutron Sources Argonne, Ill. Sept 28 -Oct 2, 1997

[9] I.M. Thorson, "Simultaneous Pulsed/Integral Neutron Facility Optimization"; Proc. ICANS-XI, Tsukuba, 1990 KEK-report 90-25 (1991) p. 463-470

[10] G.S. Bauer "The ACoM Collaboration - An International Effort to Develop Advanced Cold Moderators" to be published in Proc ICANS XIV, Starved Rock Lodge, (1998) Argonne National Laboratory

[11] K. Inoue, Y. Kiyanagi, H. Iwasa, K. Jinguji, N. Watanabe, S. Ikeda, Y. Ishikawa, Proc. ICANS-V, Jül-Conf-45 (1998)

[12] G.S. Bauer, " Some General Reflexions on "Long Pulse" Neutron Sources", J. Neut. Res., **3** (1996), pp. 253-271

[13] G.S. Bauer "Options for Neutron Scattering Instruments on Long Pulse Neutron Sources", Proc. ICANS XIII, PSI-Proceedings 95-02 (1995) pp 339-354

[14] G.S. Bauer, H. Sebening, J.-E. Vetter, H. Willax (eds.) "Realisierungsstudie zur Spallations-Neutronenquelle" report Jül-Spez-113 and KfK 3175 (1981)

[15] G.S. Bauer " The general concept for a spallation neutron source in the Federal Republic of Germany" Atomkernenergie/Kerntechnik **41**,4 (1982) pp. 234-242

[16] J. Alonso, R. Pynn. T. Russell, L. Schroeder (eds.) Proc. Workshop on Neutron Instrumentation for a Long-Pulse Spallation Source, LBL37880 / UC-406 / CONF 9504205 (1995)

[17] J. Neutron Research, (Spec. Iss.) **6** 1-3 (1997)

[18] G.S. Bauer, W.E. Fischer, U. Rohrer, U. Schryber, "Commissioning of the 1 MW Spallation Neutron Source SINQ" PAC'97, Vancouver, 12.-16. 05 1997

[19] W. Wagner, G.S. Bauer, J. Duppich, S. Janssen, E. Lehmann, M. Lüthy and H. Spitzer „Flux Measurements at the New Swiss Spallation Neutron Source SINQ" J. Neutron Research, Vol **6**, pp249-278 (1998)

[20] G.S. Bauer "Operation and Development of the New Spallation Neutron Source SINQ at the Paul Scherrer Institut" Proc. ECAART 5 , to be published in NIM

[21] F. Atchison " Neutronic Considerations in the Design of SINQ" in: Technology of Targets and Moderators for Medium to High Power Spallation Neutron Sources; PSI-Proceedings 92-03 (1992)

[22] G.S. Bauer, A. Dementyev, E. Lehmann, "Target Options for SINQ - A Neutronic Assessment" submitted to Proc ICANS XIV, Starved Rock Lodge, (1998) Argonne National Laboratory

[23] L. Ni, G S. Bauer " Heat Transfer and Thermomechanic Analyses on the Test Rods in the SINQ-Target Mark 2" to be published in Proc ICANS XIV, Starved Rock Lodge, (1998) Argonne National Laboratory

[24] A. Malik, G.S. Bauer, G. Heidenreich "Target Materials Development for SINQ and out of Beam Testing" to be published in Proc ICANS XIV, Starved Rock Lodge, (1998) Argonne National Laboratory

[25] Y. Dai, private communication: First results from materials testing of 9Cr1Mo-steel (as used for cladding the lead rods in the SINQ target) after irradiation in a mixed proton-neutron field under thermal cycling typical for accelerators, show that it still had significant ductility left even at damage levels up to more than 6 dpa.

[26] H. Heyck, B. Amrein, G.S. Bauer, K. Geissmann, " Lessons learned form the First 500 mAh of Beam on SINQ" to be published in Proc ICANS XIV, Starved Rock Lodge, (1998) Argonne National Laboratory

[27] C. Tschalär "Spallation Neutron Source at SIN" Proc. ICANS IV, KENS-report II, Tsukuba (1981) pp 56-76

[28] G.S. Bauer "Research and Development for Molten Heavy Metal Targets" Proc 2nd Int. Conf. on Accelerator-Driven Transmutation Technologies and Applications, Kalmar, H. Condé, ed. Uppsala University (1997), pp. 803-814

[29] G.S. Bauer "Spallation Neutron Source Development at the Paul Scherrer Institut" Proc. AccApp'97, ANS Ord. Nr. 700249, ISBN 0-89448-629-2 (1997) pp. 375-384

[30] G.S. Bauer, T. Broome, D. F. Filges, H. Jones, H. Lengeler, A. Letchford, G. Rees, H. Stechemesser, G. Thomas (eds.) " The European Spallation Source Study" Vol. III

[31] G.S. Bauer, F. Atchison, T.A. Broome, H.M. Conrad "A Target Development Program for Beamhole Spallation Neutron Sources in the Megawatt Range" Int. Conf. on Accelerator-Driven Transmutation Technologies and Applications, Las Vegas, July 1994 American Institute of Physics Conf. Proc. 364,(1995)105-116

[32] G.S. Bauer "Liquid Metal Target Station" report ESS-95-20-T (1995)

[33] T. Dury, B. Smith, G.S. Bauer "Design of the ESS Liquid Metal Target Using Computational Fluid Dynamics" submitted to Nuclear Technology

[34] F. Atchison, "Data and Methods for the Design of Accelerator Based Transmutation Systems"; in Proceedings of the Specialists' Meeting on Accelerator-Based Transmutation, PSI-Proceedings 92-02 (1992) p.440-498

[35] J. Duvoisin, PSI internal technical note TM-16-03 (1980)

[36] F. Atchison, PSI internal technical note TM-37-19 (1982)

[37] H. Ullmaier and F. Carsughi "Radiation damage problems in high power spallation neutron sources" Nucl. Inst. Meth. in Phys. Res. B101 (1995) 406-421

[38] K. Krautwasser, H. Derz, E. Kny, in High Temperatures and Pressures, **22**,25 (1990)

[39] S.A. Maloy, W.F. Sommer, R.D. Brown, J.E. Roberts, J. Eddleman, E. Zimmermann G. Willcutt "Progress Report on the Accelerator Production of Tritium Materials Irradiation Program" Proc. Symp. On Materials for Spallation Neutron Sources, Orlando, Fla. *TMS (1998) pp 131-138*

[40] M.W. Capiello, „Target/Blanket design for the Accelerator Production of Tritium Plant" Proc. Topical meeting on Nuc. Appl. Of Accelerator Technology, ANS .Order No 700249 , ISBN 0-89448-629-2 (1997) pp 129-135

[41] G.S. Bauer, Y. Dai and L. Ni "Experience and Research on Target and Structural Materials at PSI" Proc. Int Workshop on JHF-Science - N Arena, KEK (1998) and PSI-Bericht 98-04 (1998)

[42] S. Becker, F. Carsughi, H. Cords, H. Derz. H.J. Dietze, R. Duwe, T. Flossdorf, M. Huehnerbein, G. Kueppers, G. Pott, H. Ullmaier, T. Broome, P. Ferguson, S.A. Maloy, W.F. Sommer "Post Irradiation Investigations at the FZJ" Proc 2nd Int Workshop on Spallation Materials Technology, internal report FZ-Juelich, Jul-3450, pp 414-443

[43] F. Carsughi, H. Conrad, Y. Dai ,H. Ullmaier, "Materials Problems in Structural Target Components" to be published in a special issue of Nuclear Technology (1998)

[44] W.F. Sommer "Proton Beam Effects on W Rods, Surface cooled by Water" Proc 2nd Int Workshop on Spallation Materials Technology, internal report FZ-Juelich, Jul-3450, pp 215-229

[45] T. Broome, private communication.

[46] N. Takenaka "Cooling Water Flow Experiment for the JHF-N Arena Target" Proc. Int Workshop on JHF-Science - N Arena, KEK (1998)

[47] H. Heyck, B. Amrein, G.S. Bauer, K. Geissmann "Lessons learned form the First 500 mAh of Beam on SINQ" to be published in Proc ICANS XIV, Starved Rock Lodge, (1998) Argonne National Laboratory

[48] AUSTRON Feasibility Study; P. Bryant, M. Regler, M. Schuster, eds. BMWF, Wien (1994)

[49] G.S. Bauer "Some Aspects and Limits of Solid Metal Targets" paper presented at the AUSTRON IAC-Meeting June 30, 1998

[50] J.H. Rosenfeld, P.C. Cologer, A. Ducao and P.M. Dussinger "Heat Pipe Applications for Improved Chemical Process Unit Operations" DTX Corporation, unpublished internal report (1997)

[51] J.R. Weeks "Compatibility of Sructural Materials with Liquid Lead-Bismuth and Mercury" Proc Symp. Materials for Spallation Sources, TMS (1998) ISBN 0-87339-361-9

[52] J.F. Nejedlik and E.J. Vargo, „Kinetics of Corrosion in a Two-Phase Mercury System" Corrosion 20 (1964) pp. 384-391

[53] A.H. Fleitman and J:R: Weeks, "Mercury as a Nuclear Coolant" Nucl. Eng. Des.16 (1971),pp 266-278

[54] J.R. Weeks, "Lead, Bismuth, Tin and their Alloys as Nuclear Coolants" Nucl. Eng. Des. **15** (1971), pp 363-372

[55] Y. Orlov, private communication

[56] J:R: Weeks "On the Occurrence of Liquid Metal Embrittlement in Specific Binary Systems" private communication; BNL-internal paper 12923 (1968)

[57] E.E, Glickman, Yu.V. Goryunov, N.A. Molchanova, V.E. Panin "Life time under Load and Fracture Kinetics of Copper in the Presence of Mercury" Sov. Phys. J. SOPJAQ 24(3) (1981) pp 199-294

[58] K. Skala and G.S. Bauer "On the Pressure Wave Problem in Liquid Metal Targets" Proc. ICANS-XIII, Paul Scherrer Insitut, PSI-Proceedings 95-02 (1995)

[59] L Ni, G.S. Bauer: "Dynamic Stress of a Liquid Metal Target Container Under Pulsed Heating" submitted to ASME Journal of Pressure Vessel Technology (1998)

[60] M. North, J.H. Rosenfeld, D.B. Sarraf, G.S. Bauer and Y.Takeda"Water/Monel Heat Pipes for Cooling of Liquid Metal Targets for SINQ and ESS" Proc. ICANS-XIII, Paul Scherrer Insitut, PSI-Proceedings 95-02 (1995)

[61] F. Atchison and G. Heidenreich, "A Solid Target for SINQ based on a Pb-Shot Pebble-bed"; Proc. ICANS-XI, Tsukuba, 1990, KEK-report 90-25 (1991) p.551-568

[62] V. Kasaritsky "Feasibility Study of Technologies for Accelerator-Based Conversion of Military Plutonium and Transmutation of Long-Lived Radioactive Waste (ISTC-supported Project 17) Proc 2nd Int. Conf. on Accelerator-Driven Transmutation Technologies and Applications, Kalmar, H. Condé, ed. Uppsala University (1997), pp. 77-90

[63] http//www.pns.anl.gov/icans/icansdescript.html

[64] T. Mukaiyama, Y. Oyama, M.Mitsumoto, T.Takakazu, R. Hino"Neutron Science Project at JAERI" Proc. Top. Meetg. Nucl. App. Acc. Tech. ANS (1997), ISBN 0-89448-629-2; pp 398-404

[65] G.S. Bauer, J. Hastings, N. Watanabe, in preparation

[66] G.S. Bauer "The ACoM Collaboration - An International Effort to Develop Advanced Cold Moderators" to be published in Proc ICANS XIV, Starved Rock Lodge, (1998) Argonne National Laboratory

[67] G.S. Bauer, Y. Dai and L.Ni "Experience and Research on Target and Structural Materials at PSI "Proc. Int Workshop on JHF-Scienc N-Arena KEK (1998) and PSI-Bericht 98-04

[68] S.F. Sidorkin, G.S Bauer , Y. Dai , M.I. Grachev, L.V. Kravchuk., Y.I. Orlov; "Opportunities for Irradiation Studies of Structural Materials for Neutron Sources at the Proton Beam-Stop of Moscow Meson Factory" paper presented at ICANS-XIV Starved Rock Lodge, Utica Ill., USA June 14-19, 1998

[69] Y. Dai "Research Activities at PSI on Structural Materials for Spallation Neutron Sources" Proc 2nd Int Workshop on Spallation Materials Technology, internal report FZ-Juelich, Jul-3450, pp 265-295